

An Optimal Control Approach to the Persistent Monitoring Problem

- Technical Report -

Christos.G. Cassandras, Xuchao Lin and Xu Chu Ding*

Division of Systems Engineering
and Center for Information and Systems Engineering
Boston University, cgc@bu.edu, mmxclin@bu.edu, xcding@bu.edu

January 2012

Abstract

We propose an optimal control framework for persistent monitoring problems where the objective is to control the movement of mobile nodes to minimize an uncertainty metric in a given mission space. For multi agent in a one-dimensional mission space, we show that the optimal solution is obtained in terms of a sequence of switching locations and waiting time on these switching points, thus reducing it to a parametric optimization problem. Using Infinitesimal Perturbation Analysis (IPA) we obtain a complete solution through a gradient-based algorithm. We also discuss a receding horizon controller which is capable of obtaining a near-optimal solution on-the-fly.

1 Introduction

Enabled by recent technological advances, the deployment of autonomous agents that can cooperatively perform complex tasks is rapidly becoming a reality. In particular, there has been considerable progress reported in the literature on robotics and sensor networks regarding coverage control [1–3], surveillance [4, 5] and environmental sampling [6, 7] missions. In this paper, we are interested in generating optimal control strategies for *persistent monitoring* tasks; these arise when agents must monitor a dynamically changing environment which cannot be fully covered by a stationary team of available agents. Persistent monitoring differs from traditional coverage tasks due to the perpetual need to cover a changing environment, i.e., all areas of the mission space must be visited infinitely often. The main challenge in designing control strategies in this case is in balancing the presence of agents in the changing environment so that it is covered over time optimally (in some well-defined sense) while still satisfying

*The authors' work is supported in part by NSF under Grant EFRI-0735974, by AFOSR under grant FA9550-09-1-0095, by DOE under grant DE-FG52-06NA27490, by ONR under grant N00014-09-1-1051 and by ARO under grant W911NF-11-1-0227.

sensing and motion constraints. Examples of persistent monitoring missions include surveillance and theft prevention in a building, patrol missions with unmanned vehicles, and environmental applications where routine sampling of an area is involved.

In this paper, we address the persistent monitoring problem by proposing an optimal control framework to drive agents so as to minimize a metric of uncertainty over the environment. In coverage control [2,3], it is common to model knowledge of the environment as a non-negative density function defined over the mission space, and usually assumed to be fixed over time. However, since persistent monitoring tasks involve dynamically changing environments, it is natural to extend it to a function of both space and time to model uncertainty in the environment. We assume that uncertainty at a point grows in time if it is not covered by any agent sensors. To model sensor coverage, we define a probability of detecting events at each point of the mission space by agent sensors. Thus, the uncertainty of the environment decreases with a rate proportional to the event detection probability, i.e., the higher the sensing effectiveness is, the faster the uncertainty is reduced..

While it is desirable to track the value of uncertainty over all points in the environment, this is generally infeasible due to computational complexity and memory constraints. Motivated by polling models in queueing theory, e.g., spatial queueing [8], [9], and by stochastic flow models [10], we assign sampling points of the environment to be monitored persistently (this is equivalent to partitioning the environment into a discrete set of regions.) We associate to these points “uncertainty queues” which are visited by one or more “servers”. The growth in uncertainty at a sampling point can then be viewed as a flow into a queue, and the reduction in uncertainty (when covered by an agent) can be viewed as the queue being visited by mobile servers as in a polling system. Moreover, the service flow rates depend on the distance of the sampling point to nearby agents. From this point of view, we aim to control the movement of the servers (agents) so that the total accumulated “uncertainty queue” content is minimized.

Control and motion planning for agents performing persistent monitoring tasks have been studied in the literature. In [1] the focus is on sweep coverage problems, where agents are controlled to sweep an area. In [6, 11] a similar metric of uncertainty is used to model knowledge of a dynamic environment. In [11], the sampling points in a 1-dimensional environment are denoted as cells, and the optimal control policy for a two-cell problem is given. Problems with more than two cells are addressed by a heuristic policy. In [6], the authors proposed a stabilizing speed controller for a single agent so that the accumulated uncertainty over a given path in the environment is bounded, along with an optimal controller that minimizes the maximum steady-state uncertainty, assuming that the agent travels along a closed path and does not change direction. The persistent monitoring problem is also related to robot patrol problems, where a team of robots are required to visit points in the workspace with frequency constraints [12–14].

Our ultimate goal is to optimally control a team of cooperating agents in a 2 or 3-dimensional environment. The contribution of this paper is to take a first step toward this goal by formulating and solving an optimal control problem for a team of agents moving in a 1-dimensional mission space described by an interval $[0, L] \subset \mathbb{R}$ in which we minimize the accumulated uncertainty over a given time horizon and over an arbitrary number of sampling points. Even in this simple case, determining a complete explicit solution is computationally hard. However, we show that the problem can be reduced to a *parametric* optimization problem. In particular, the optimal trajectory of each agent is to move at full speed until it reaches some switching point, dwell on the switching point for some time (possibly zero), and then switch directions. In addition, we prove that all agents should never reach the end points of the mis-

sion space $[0, L]$. Thus, each agent’s optimal trajectory is fully described by a set of switching points $\{\theta_1, \dots, \theta_K\}$ and associated waiting times at these points, $\{w_1, \dots, w_K\}$. As a result, we show that the behavior of the agents operating under optimal control is described by a hybrid system. This allows us to make use of generalized Infinitesimal Perturbation Analysis (IPA), as presented in [15], [16], to determine gradients of the objective function with respect to these parameters and subsequently obtain optimal switching locations and waiting times that fully characterize an optimal solution. It also allows us to exploit robustness properties of IPA to extend this solution approach to a stochastic uncertainty model. Our analysis establishes the basis for extending this approach to a 2-dimensional mission space (in ongoing research). In a broader context, our approach brings together optimal control, hybrid systems, and perturbation analysis techniques in solving a class of problems which, under optimal control, can be shown to behave like hybrid systems characterized by a set of parameters whose optimal values deliver a complete optimal control solution.

The rest of the paper is organized as follows. Section 2 formulates the optimal control problem. Section 3 characterizes the solution of the optimal control problem in terms of two parameter vectors specifying switching points in the mission space and associated dwelling times at them. Using IPA in conjunction with a gradient-based algorithm, a complete solution is also provided. Section 4 provides some numerical results and Section 5 concludes the paper.

2 Persistent Monitoring Problem Formulation

We consider N mobile agents moving in a 1-dimensional mission space of length L , for simplicity taken to be an interval $[0, L] \subset \mathbb{R}$. Let the position of the agents at time t be $s_n(t) \in [0, L]$, $n = 1, \dots, N$, following the dynamics:

$$\dot{s}_n(t) = u_n(t) \tag{1}$$

i.e., we assume that the agent can control its direction and speed. Without loss of generality, after some rescaling with the size of the mission space L , we further assume that the speed is constrained by $|u_n(t)| \leq 1$, $n = 1, \dots, N$. For the sake of generality, we include the additional constraint:

$$a \leq s(t) \leq b, \quad a \geq 0, \quad b \leq L \tag{2}$$

over all t to allow for mission spaces where the agents may not reach the end points of $[0, L]$, possibly due to the presence of obstacles. We also point out that the agent dynamics in (1) can be replaced by a more general model of the form $\dot{s}_n(t) = g_n(s_n) + b_n u_n(t)$ without affecting the main results of our analysis (see also Remark 1 in Section 3.1.) Finally, an additional constraint may be imposed if we assume that the agents are initially located so that $s_n(0) < s_{n+1}(0)$, $n = 1, \dots, N - 1$, and we wish to prevent them from subsequently crossing each other over all t :

$$s_n(t) - s_{n+1}(t) \leq 0 \tag{3}$$

We associate with every point $x \in [0, L]$ a function $p_n(x, s_n)$ that measures the probability that an event at location x is detected by agent n . We also assume that $p_n(x, s_n) = 1$ if $x = s_n$, and that $p_n(x, s_n)$ is monotonically nonincreasing in the distance $|x - s_n|$ between x and s_n , thus capturing the reduced effectiveness of a sensor over its range which we consider to be finite and denoted by r_n (this is the same as the concept of “sensor footprint” found in the robotics literature.) Therefore, we set $p_n(x, s_n) = 0$

when $|x - s_n| > r_n$. Although our analysis is not affected by the precise sensing model $p_n(x, s_n)$, we will limit ourselves to a linear decay model as follows:

$$p_n(x, s_n) = \begin{cases} 1 - \frac{|x - s_n|}{r_n}, & \text{if } |x - s_n| \leq r_n \\ 0, & \text{if } |x - s_n| > r_n \end{cases} \quad (4)$$

Next, consider a set of points $\{\alpha_i\}$, $i = 1, \dots, M$, $\alpha_i \in [0, L]$, and associate a time-varying measure of uncertainty with each point α_i , which we denote by $R_i(t)$. Without loss of generality, we assume $0 \leq \alpha_1 \leq \dots \leq \alpha_M \leq L$ and, to simplify notation, we set $p_{n,i}(s_n(t)) \equiv p_n(\alpha_i, s_n(t))$. This set may be selected to contain points of interest in the environment, or sampled points from the mission space. Alternatively, we may consider a partition of $[0, L]$ into M intervals whose center points are $\alpha_i = \frac{(2i-1)L}{2M}$, $i = 1, \dots, M$. We can then set $p_n(x, s_n(t)) = p_{n,i}(s_n(t))$ for all $x \in [\alpha_i - \frac{L}{2M}, \alpha_i + \frac{L}{2M}]$. Therefore, the joint probability of detecting an event at location $x \in [\alpha_i - \frac{L}{2M}, \alpha_i + \frac{L}{2M}]$ by all the N agents simultaneously (assuming detection independence) is:

$$P_i(\mathbf{s}(t)) = 1 - \prod_{n=1}^Q [1 - p_{n,i}(s_n(t))] \quad (5)$$

where we set $\mathbf{s}(t) = [s_1(t), \dots, s_N(t)]^T$. We define uncertainty functions $R_i(t)$ associated with the intervals $[\alpha_i - \frac{L}{2M}, \alpha_i + \frac{L}{2M}]$, $i = 1, \dots, M$, so that they have the following properties: (i) $R_i(t)$ increases with a prespecified rate A_i if $P_i(\mathbf{s}(t)) = 0$, (ii) $R_i(t)$ decreases with a fixed rate B if $P_i(\mathbf{s}(t)) = 1$ and (iii) $R_i(t) \geq 0$ for all t . It is then natural to model uncertainty so that its decrease is proportional to the probability of detection. In particular, we model the dynamics of $R_i(t)$, $i = 1, \dots, M$, as follows:

$$\dot{R}_i(t) = \begin{cases} 0 & \text{if } R_i(t) = 0, A_i \leq BP_i(\mathbf{s}(t)) \\ A_i - BP_i(\mathbf{s}(t)) & \text{otherwise} \end{cases} \quad (6)$$

where we assume that initial conditions $R_i(0)$, $i = 1, \dots, M$, are given and that $B > A_i > 0$ (thus, the uncertainty strictly decreases when there is perfect sensing $P_i(\mathbf{s}(t)) = 1$.)

Viewing persistent monitoring as a polling system, each point α_i (equivalently, i th interval in $[0, L]$) is associated with a “virtual queue” where uncertainty accumulates with inflow rate A_i . The service rate of this queue is time-varying and given by $BP_i(\mathbf{s}(t))$, controllable through the agent position at time t . Figure 1 illustrates this polling system when $N = 1$. This interpretation is convenient for characterizing the *stability* of such a system over a mission time T : For each queue, we may require that $\int_0^T A_i < \int_0^T BP_i(s(t))dt$. Alternatively, we may require that each queue becomes empty at least once over $[0, T]$. We may also impose conditions such as $R_i(T) \leq R_{\max}$ for each queue as additional constraints for our problem so as to provide bounded uncertainty guarantees, although we will not do so in this paper. Note that this analogy readily extends to 2 or 3-dimensional settings.

The goal of the optimal persistent monitoring problem we consider is to control the movement of the N agents through $u_n(t)$ in (1) so that the cumulative uncertainty over all sensing points $\{\alpha_i\}$, $i = 1, \dots, M$ is minimized over a fixed time horizon T . Thus, setting $\mathbf{u}(t) = [u_1(t), \dots, u_N(t)]$ we aim to solve the following optimal control problem **P1**:

$$\min_{\mathbf{u}(t)} J = \frac{1}{T} \int_0^T \sum_{i=1}^M R_i(t) dt \quad (7)$$

subject to the agent dynamics (1), uncertainty dynamics (6), control constraint $|u_n(t)| \leq 1$, $t \in [0, T]$, and state constraints (2), $t \in [0, T]$. Note that we require $a \leq r_n$ and $b \geq L - r_m$, for at least some

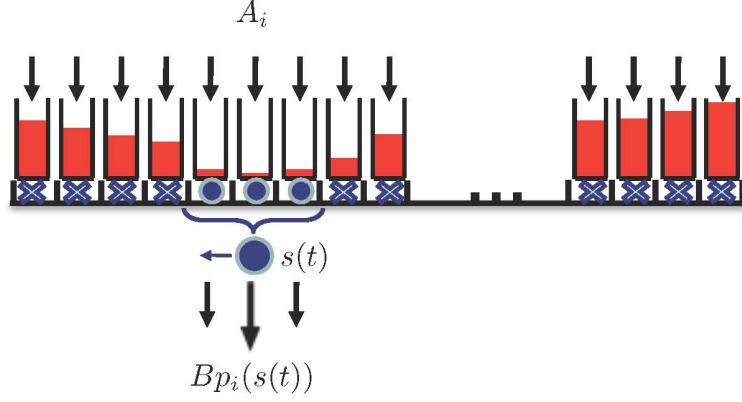


Figure 1: A queuing system analog of the persistent monitoring problem.

$n, m = 1, \dots, N$; this is to ensure that there are no points in $[0, L]$ which can never be sensed, i.e., any i such that $\alpha_i < a - r_n$ or $\alpha_i > b + r_n$ would always lie outside any agent's sensing range. We will omit the additional constraint (3) from our initial analysis, but we will show that, when it is included, the optimal solution never allows it to be active.

3 Optimal Control Solution

3.1 Hamiltonian analysis

We first characterize the optimal control solution of problem **P1** and show that it can be reduced to a parametric optimization problem. This allows us to utilize an Infinitesimal Perturbation Analysis (IPA) gradient estimation approach [15] to find a complete optimal solution through a gradient-based algorithm. We define the state vector $\mathbf{x}(t) = [s_1(t), \dots, s_N(t), R_1(t), \dots, R_M(t)]^T$ and the associated costate vector $\lambda(t) = [\lambda_{s_1}(t), \dots, \lambda_{s_N}(t), \lambda_1(t), \dots, \lambda_M(t)]^T$. In view of the discontinuity in the dynamics of $R_i(t)$ in (6), the optimal state trajectory may contain a boundary arc when $R_i(t) = 0$ for any i ; otherwise, the state evolves in an interior arc. We first analyze the system operating in such an interior arc and omit the constraint (2) as well. Using (1) and (6), the Hamiltonian is

$$H(\mathbf{x}, \lambda, \mathbf{u}) = \sum_{i=1}^M R_i(t) + \sum_{n=1}^N \lambda_{s_n}(t) u_n(t) + \sum_{i=1}^M \lambda_i(t) \dot{R}_i(t) \quad (8)$$

and the costate equations $\dot{\lambda} = -\frac{\partial H}{\partial \mathbf{x}}$ are

$$\dot{\lambda}_i(t) = -\frac{\partial H}{\partial R_i(t)} = -1, \quad i = 1, \dots, M \quad (9)$$

$$\dot{\lambda}_{s_n}(t) = -\frac{\partial H}{\partial s_n(t)} = -\frac{B}{r_n} \sum_{i \in F_n^-(t)} \lambda_i(t) \prod_{d \neq n} [1 - p_{d,i}(s_d(t))] + \frac{B}{r_n} \sum_{i \in F_n^+(t)} \lambda_i(t) \prod_{d \neq n} [1 - p_{d,i}(s_d(t))] \quad (10)$$

where we have used (4), and the sets $F_n^-(t)$ and $F_n^+(t)$ are defined as

$$\begin{aligned} F_n^-(t) &= \{i : s_n(t) - r_n \leq \alpha_i \leq s_n(t)\} \\ F_n^+(t) &= \{i : s_n(t) < \alpha_i \leq s_n(t) + r_n\} \end{aligned} \quad (11)$$

for $n = 1, \dots, N$. Note that $F_n^-(t)$, $F_n^+(t)$ identify all points α_i to the left and right of $s_n(t)$ respectively that are within agent n 's sensing range. Since we impose no terminal state constraints, the boundary conditions are $\lambda_i(T) = 0$, $i = 1, \dots, M$ and $\lambda_{s_n}(T) = 0$, $n = 1, \dots, N$. Applying the Pontryagin minimum principle to (8) with $\mathbf{u}^*(t)$, $t \in [0, T)$, denoting an optimal control, we have

$$H(\mathbf{x}^*, \boldsymbol{\lambda}^*, \mathbf{u}^*) = \min_{u_n \in [-1, 1], n=1, \dots, N} H(\mathbf{x}, \boldsymbol{\lambda}, \mathbf{u})$$

and it is immediately obvious that it is necessary for an optimal control to satisfy:

$$u_n^*(t) = \begin{cases} 1 & \text{if } \lambda_{s_n}(t) < 0 \\ -1 & \text{if } \lambda_{s_n}(t) > 0 \end{cases} \quad (12)$$

This condition excludes the possibility that $\lambda_{s_n}(t) = 0$ over some finite singular intervals [17]. We will show that if $s_n(t) = a > 0$ or $s_n(t) = b < L$, then $\lambda_{s_n}(t) = 0$ for some $n \in \{1, \dots, N\}$ may in fact exist for some finite arc; otherwise $\lambda_{s_n}(t) = 0$ can arise only when $u_n(t) = 0$.

The implication of (9) with $\lambda_i(T) = 0$ is that $\lambda_i(t) = T - t$ for all $t \in [0, T]$ and all $i = 1, \dots, M$ and that $\lambda_i(t)$ is monotonically decreasing starting with $\lambda_i(0) = T$. However, this is only true if the entire optimal trajectory is an interior arc, i.e., all $R_i(t) \geq 0$ constraints for all $i = 1, \dots, M$ remain inactive. On the other hand, looking at (10), observe that when the two end points, 0 and L , are not within the range of an agent, we have $|F_n^-(t)| = |F_n^+(t)|$, since the number of indices i satisfying $s_n(t) - r_n \leq \alpha_i \leq s_n(t)$ is the same as that satisfying $s_n(t) < \alpha_i \leq s_n(t) + r_n$. Consequently, for the one-agent case $N = 1$, (10) becomes

$$\dot{\lambda}_{s_1}(t) = -\frac{B}{r_1} \sum_{i \in F_1^-(t)} \lambda_i(t) + \frac{B}{r_1} \sum_{i \in F_1^+(t)} \lambda_i(t) \quad (13)$$

and $\dot{\lambda}_{s_1}(t) = 0$ since the two terms in (13) will cancel out, i.e., $\lambda_{s_1}(t)$ remains constant as long as this condition is satisfied and, in addition, none of the state constraints $R_i(t) \geq 0$, $i = 1, \dots, M$, is active. Thus, for the one agent case, as long as the optimal trajectory is an interior arc and $\lambda_{s_1}(t) < 0$, the agent moves at maximal speed $u_1^*(t) = 1$ in the positive direction towards the point $s_1 = b$. If $\lambda_{s_1}(t)$ switches sign before any of the state constraints $R_i(t) \geq 0$, $i = 1, \dots, M$, becomes active or the agent reaches the end point $s_1 = b$, then $u_1^*(t) = -1$ and the agent reverses its direction or, possibly, comes to rest.

In what follows, we examine the effect of the state constraints which significantly complicates the analysis, leading to a challenging two-point-boundary-value problem. However, we will establish the fact that the complete solution boils down to determining a set of switching locations over $[a, b]$ and waiting times at these switching points, with the end points, 0 and L , being always infeasible on an optimal trajectory. This is a much simpler problem that we are subsequently able to solve.

We begin by recalling that the dynamics in (6) indicate a discontinuity arising when the condition $R_i(t) = 0$ is satisfied while $\dot{R}_i(t) = A_i - BP_i(\mathbf{s}(t)) < 0$ for some $i = 1, \dots, M$. Thus, $R_i = 0$ defines an interior boundary condition which is not an explicit function of time. Following standard optimal control analysis [17], if this condition is satisfied at time t for some $j \in \{1, \dots, M\}$,

$$H(\mathbf{x}(t^-), \boldsymbol{\lambda}(t^-), \mathbf{u}(t^-)) = H(\mathbf{x}(t^+), \boldsymbol{\lambda}(t^+), \mathbf{u}(t^+)) \quad (14)$$

where we note that one can choose to set the Hamiltonian to be continuous at the entry point of a boundary arc or at the exit point. Using (8) and (6), (14) implies:

$$\sum_{n=1}^N \lambda_{s_n}^*(t^-) u_n^*(t^-) + \lambda_j^*(t^-) [A_j(t) - BP_j(\mathbf{s}(t))] = \sum_{n=1}^N \lambda_{s_n}^*(t^+) u_n^*(t^+) \quad (15)$$

In addition, $\lambda_{s_n}^*(t^-) = \lambda_{s_n}^*(t^+)$ for all $n = 1, \dots, N$ and $\lambda_i^*(t^-) = \lambda_i^*(t^+)$ for all $i \neq j$, but $\lambda_j^*(t)$ may experience a discontinuity so that:

$$\lambda_j^*(t^-) = \lambda_j^*(t^+) - \pi_j \quad (16)$$

where $\pi_j \geq 0$ is a multiplier associated with the constraint $-R_j(t) \leq 0$. Recalling (12), since $\lambda_{s_n}^*(t)$ remains unaffected, so does the optimal control, i.e., $u_n^*(t^-) = u_n^*(t^+)$. Moreover, since this is an entry point of a boundary arc, it follows from (6) that $A_j - BP_j(\mathbf{s}(t)) < 0$. Therefore, (15) and (16) imply that

$$\lambda_j^*(t^-) = 0, \quad \lambda_j^*(t^+) = \pi_j \geq 0.$$

Thus, $\lambda_i(t)$ always decreases with constant rate -1 until $R_i(t) = 0$ is active, at which point $\lambda_i(t)$ jumps to a non-negative value π_i and decreases with rate -1 again. The value of π_i is determined by how long it takes for the agents to reduce $R_i(t)$ to 0 once again. Obviously,

$$\lambda_i(t) \geq 0, \quad i = 1, \dots, M, \quad t \in [0, T] \quad (17)$$

with equality holding only if $t = T$, or $t = t_0^-$ with $R_i(t_0) = 0$, $R_i(t') > 0$, where $t' \in [t_0 - \delta, t_0)$, $\delta > 0$. The actual evaluation of the costate vector over the interval $[0, T]$ requires solving (10), which in turn involves the determination of all points where the state variables $R_i(t)$ reach their minimum feasible values $R_i(t) = 0$, $i = 1, \dots, M$. This generally involves the solution of a two-point-boundary-value problem. However, our analysis thus far has already established the structure of the optimal control (12) which we have seen to remain unaffected by the presence of boundary arcs when $R_i(t) = 0$ for one or more $i = 1, \dots, M$. We will next prove some additional structural properties of an optimal trajectory, based on which we show that it is fully characterized by a set of non-negative scalar parameters. Determining the values of these parameters is a much simpler problem that does not require the solution of a two-point-boundary-value problem.

Let us turn our attention to the constraints $s_n(t) \geq a$ and $s_n(t) \leq b$ and consider first the case where $a = 0$, $b = L$, i.e., the agents can move over the entire $[0, L]$. We shall make use of the following technical condition:

Assumption 1: For any $n = 1, \dots, N$, $i = 1, \dots, M$, $t \in (0, T)$, and any $\varepsilon > 0$, if $s_n(t) = 0$, $s_n(t - \varepsilon) > 0$, then either $R_i(\tau) > 0$ for all $\tau \in [t - \varepsilon, t]$ or $R_i(\tau) = 0$ for all $\tau \in [t - \varepsilon, t]$; if $s_n(t) = L$, $s_n(t - \varepsilon) < L$, then either $R_i(\tau) > 0$ for all $\tau \in [t - \varepsilon, t]$ or $R_i(\tau) = 0$ for all $\tau \in [t - \varepsilon, t]$.

This condition excludes the case where an agent reaches an endpoint of the mission space at the exact same time that any one of the uncertainty functions reaches its minimal value of zero. Then, the following proposition asserts that neither of the constraints $s_n(t) \geq 0$ and $s_n(t) \leq L$ can become active on an optimal trajectory.

Proposition 3.1 *Under Assumption 1, if $a = 0$, $b = L$, then on an optimal trajectory: $s_n^*(t) \neq 0$ and $s_n^*(t) \neq L$ for all $t \in (0, T)$, $n \in \{1, \dots, N\}$.*

Proof. Suppose at $t = t_0 < T$ an agent reaches the left endpoint, i.e., $s_n^*(t_0) = 0, s_n^*(t_0^-) > 0$. We will then establish a contradiction. Thus, assuming $s_n^*(t_0) = 0$, we first show that $\lambda_{s_n}^*(t_0^-) = 0$ by a contradiction argument. Assume that $\lambda_{s_n}^*(t_0^-) \neq 0$, in which case, since the agent is moving toward $s_n = 0$, we have $u_n^*(t_0^-) = -1$ and $\lambda_{s_n}^*(t_0^-) > 0$ from (12). Then, $\lambda_{s_n}^*(t)$ may experience a discontinuity so that

$$\lambda_{s_n}^*(t_0^-) = \lambda_{s_n}^*(t_0^+) - \pi_n \quad (18)$$

where $\pi_n \geq 0$ is a scalar constant. It follows that $\lambda_{s_n}^*(t_0^+) = \lambda_{s_n}^*(t_0^-) + \pi_n > 0$. Since the constraint $s_n(t) = 0$ is not an explicit function of time, we have

$$\lambda_{s_n}^*(t_0^-) u_n^*(t_0^-) = \lambda_{s_n}^*(t_0^+) u_n^*(t_0^+) \quad (19)$$

On the other hand, $u_n^*(t_0^+) \geq 0$, since agent n must either come to rest or reverse its motion at $s_n = 0$, hence $\lambda_{s_n}^*(t_0^+) u_n^*(t_0^+) \geq 0$. This violates (19), since $\lambda_{s_n}^*(t_0^-) u_n^*(t_0^-) < 0$. This contradiction implies that $\lambda_{s_n}^*(t_0^-) = 0$. Next, consider (10) and observe that in (11) we have $F_n^-(t_0) = \emptyset$, since $\alpha_i > s_n^*(t_0) = 0$ for all $i = 1, \dots, M$. Therefore, recalling (17), it follows from (10) that

$$\dot{\lambda}_{s_n}^*(t_0^-) = \frac{B}{r_n} \sum_{i \in F_n^+(t_0^-)} \lambda_i(t_0^-) \prod_{d \neq n} [1 - p_{d,i}(s_d(t_0^-))] \geq 0$$

Under Assumption 1, there exists $\delta_1 > 0$ such that during the interval $(t_0 - \delta_1, t_0)$ no $R_i(t) \geq 0$ becomes active, hence no $\lambda_i(t)$ encounters a jump for $i = 1, \dots, M$. It follows that $\lambda_i^*(t) > 0$ for $i \in F_n^+(t)$ and $\dot{\lambda}_{s_n}^*(t)$ is continuous with $\dot{\lambda}_{s_n}^*(t) > 0$ for $t \in (t_0 - \delta_1, t_0)$. Again, since $s_n^*(t_0) = 0$, there exists some $\delta_2 \leq \delta_1$ such that for $t \in (t_0 - \delta_2, t_0)$, we have $u_n^*(t) < 0$ and $\lambda_{s_n}^*(t) \geq 0$. Thus, for $t \in (t_0 - \delta_2, t_0)$, we have $\lambda_{s_n}^*(t) \geq 0$ and $\dot{\lambda}_{s_n}^*(t) > 0$. This contradicts the fact we already established that $\lambda_{s_n}^*(t_0^-) = 0$ and we conclude that $s_n^*(t) \neq 0$ for all $t \in [0, T]$, $n = 1, \dots, N$. Using a similar line of argument, we can also show that $s_n^*(t) \neq L$. ■

Proposition 3.2 *If $a > 0$ and (or) $b < L$, then on an optimal trajectory there exist finite length intervals $[t_0, t_1]$ such that $s_n(t) = a$ and (or) $s_n(t) = b$, for some $n \in \{1, \dots, N\}$, $t \in [t_0, t_1]$, $0 \leq t_0 < t_1 \leq T$.*

Proof. Proceeding as in the proof of Proposition 3.1, when $s_n^*(t_0) = a$ we can establish (19) and the fact that $\lambda_{s_n}^*(t_0^-) = 0$. On the other hand, $u_n^*(t_0^+) \geq 0$, since the agent must either come to rest or reverse its motion at $s_n(t_0) = a$. In other words, when $s_n(t_0) = a$ on an optimal trajectory, (19) is satisfied either with the agent reversing its direction immediately (in which case $t_1 = t_0$ and $\lambda_{s_n}^*(t_0^+) = 0$) or staying on the boundary arc for a finite time interval (in which case $t_1 > t_0$ and $u_n^*(t) = 0$ for $t \in [t_0, t_1]$). The exact same argument can be applied to $s_n(t) = b$. ■

The next result establishes the fact that on an optimal trajectory, every agent either moves at full speed or is at rest.

Proposition 3.3 *On an optimal trajectory, either $u_n^*(t) = \pm 1$ if $\lambda_{s_n}^*(t) \neq 0$, or $u_n^*(t) = 0$ if $\lambda_{s_n}^*(t) = 0$ for $t \in [0, T]$, $n = 1, \dots, N$.*

Proof. When $\lambda_{s_n}^*(t) \neq 0$, we have shown in (12) that $u_n^*(t) = \pm 1$, depending on the sign of $\lambda_{s_n}^*(t)$. Thus, it remains to consider the case $\lambda_{s_n}^*(t) = 0$ for some $t \in [t_1, t_2]$, where $0 \leq t_1 < t_2 \leq T$. Since the state is

in a singular arc, $\lambda_{s_n}^*(t)$ does not provide information about $u_n^*(t)$. On the other hand, the Hamiltonian in (8) is not an explicit function of time, therefore, setting $H(\mathbf{x}^*, \lambda^*, \mathbf{u}^*) \equiv H^*$, we have $\frac{dH^*}{dt} = 0$, which gives

$$\frac{dH^*}{dt} = \sum_{i=1}^M \dot{R}_i^*(t) + \sum_{n=1}^N \dot{\lambda}_{s_n}^*(t) u_n^*(t) + \sum_{n=1}^N \lambda_{s_n}^*(t) \dot{u}_n^*(t) + \sum_{i=1}^M \dot{\lambda}_i^*(t) \dot{R}_i^*(t) + \sum_{i=1}^M \lambda_i^*(t) \ddot{R}_i^*(t) = 0 \quad (20)$$

Define $S(t) = \{n | \lambda_{s_n}(t) = 0, n = 1, \dots, N\}$ as the set of indices of agents that are in a singular arc and $\bar{S}(t) = \{n | \lambda_{s_n}(t) \neq 0, n = 1, \dots, N\}$ as the set of indices of all other agents. Thus, $\lambda_{s_n}^*(t) = 0$, $\dot{\lambda}_{s_n}^*(t) = 0$ for $t \in [t_1, t_2]$, $n \in S(t)$. In addition, agents move with constant full speed, either 1 or -1 , so that $\dot{u}_n^*(t) = 0$, $n \in \bar{S}(t)$. Then, (20) becomes

$$\frac{dH^*}{dt} = \sum_{i=1}^M [1 + \dot{\lambda}_i^*(t)] \dot{R}_i^*(t) + \sum_{n \in \bar{S}(t)} \dot{\lambda}_{s_n}^*(t) u_n^*(t) + \sum_{i=1}^M \lambda_i^*(t) \ddot{R}_i^*(t) = 0 \quad (21)$$

From (9), $\dot{\lambda}_i^*(t) = -1$, $i = 1, \dots, M$, so $1 + \dot{\lambda}_i^*(t) = 0$, leaving only the last two terms above. Note that $\dot{\lambda}_{s_n}^*(t) = -\frac{\partial H^*}{\partial s_n^*(t)}$ and writing $\ddot{R}_i^*(t) = \frac{d\dot{R}_i^*(t)}{dt}$ we get:

$$-\sum_{n \in \bar{S}(t)} u_n^*(t) \frac{\partial H^*}{\partial s_n^*(t)} + \sum_{i=1, R_i \neq 0}^M \lambda_i^*(t) \frac{d\dot{R}_i^*(t)}{dt} = 0$$

Recall from (6) that when $R_i(t) \neq 0$ we have $\dot{R}_i(t) = A_i - B[1 - \prod_{n=1}^N [1 - p_i(s_n(t))]]$, so that

$$\begin{aligned} \frac{\partial H^*}{\partial s_n^*(t)} &= -B \sum_{i=1, R_i \neq 0}^M \lambda_i^*(t) \frac{\partial p_i(s_n^*(t))}{\partial s_n^*(t)} \prod_{d \neq n}^N (1 - p_i(s_d^*(t))) \\ \frac{d\dot{R}_i^*(t)}{dt} &= -B \sum_{n=1}^N u_n^*(t) \frac{\partial p_i(s_n^*(t))}{\partial s_n^*(t)} \prod_{d \neq n}^N (1 - p_i(s_d^*(t))) \end{aligned}$$

which results in

$$\begin{aligned} & B \sum_{i=1, R_i \neq 0}^M \lambda_i^*(t) \left[\sum_{n \in \bar{S}(t)} u_n^*(t) \frac{\partial p_i(s_n^*(t))}{\partial s_n^*(t)} \prod_{d \neq n}^N (1 - p_i(s_d^*(t))) - \sum_{n=1}^N u_n^*(t) \frac{\partial p_i(s_n^*(t))}{\partial s_n^*(t)} \prod_{d \neq n}^N (1 - p_i(s_d^*(t))) \right] \\ &= -B \sum_{i=1, R_i \neq 0}^M \lambda_i^*(t) \sum_{n \in S(t)} u_n^*(t) \frac{\partial p_i(s_n^*(t))}{\partial s_n^*(t)} \prod_{d \neq n}^N (1 - p_i(s_d^*(t))) = 0 \end{aligned} \quad (22)$$

Note that $\frac{\partial p_i(s_1^*(t))}{\partial s_1^*(t)} = \pm \frac{1}{r_1}$ or 0, depending on the relative position of $s_1^*(t)$ with respect to α_i . Moreover, (22) is invariant to M or the precise way in which the mission space $[0, L]$ is partitioned, which implies that

$$\lambda_i^*(t) \sum_{n \in S(t)} u_n^*(t) \frac{\partial p_i(s_n^*(t))}{\partial s_n^*(t)} \prod_{d \neq n}^N (1 - p_i(s_d^*(t))) = 0$$

for all $i = 1, \dots, M$, $t \in [t_1, t_2]$. Since $\dot{\lambda}_i^*(t) = -1$, $i = 1, \dots, M$, it is clear that to satisfy this equality we must have $u_n^*(t) = 0$ for all $t \in [t_1, t_2]$, $n \in S(t)$. In conclusion, in a singular arc with $\lambda_{s_n}^*(t) = 0$ for some $n \in \{1, \dots, N\}$, the optimal control is $u_n^*(t) = 0$. ■

Next, we consider the case where the additional state constraint (3) is included. We can then prove that this constraint is never active on an optimal trajectory, i.e., agents reverse their direction before making contact with any other agent.

Proposition 3.4 *If the constraint (3) is included in problem **PI**, then on an optimal trajectory, $s_n^*(t) \neq s_{n+1}^*(t)$ for $t \in (0, T]$, $n = 1, \dots, N-1$.*

Proof. Suppose at $t = t_0 < T$ we have $s_n^*(t_0) = s_{n+1}^*(t_0)$, for some $n = 1, \dots, N-1$. We will then establish a contradiction. First assuming that both agents are moving (as opposed to one being at rest) toward each other, we have $u_n^*(t_0^-) = 1$ and $u_{n+1}^*(t_0^-) = -1$. From (12) and Prop 3.3, we know $\lambda_{s_n}^*(t_0^-) < 0$ and $\lambda_{s_{n+1}}^*(t_0^-) > 0$. When the constraint $s_n(t) - s_{n+1}(t) \leq 0$ is active, $\lambda_{s_n}^*(t)$ and $\lambda_{s_{n+1}}^*(t)$ may experience a discontinuity so that

$$\lambda_{s_n}^*(t_0^-) = \lambda_{s_n}^*(t_0^+) + \pi \quad (23)$$

$$\lambda_{s_{n+1}}^*(t_0^-) = \lambda_{s_{n+1}}^*(t_0^+) - \pi \quad (24)$$

where $\pi \geq 0$ is a scalar constant. It follows that $\lambda_{s_n}^*(t_0^+) = \lambda_{s_n}^*(t_0^-) - \pi < 0$ and $\lambda_{s_{n+1}}^*(t_0^+) = \lambda_{s_{n+1}}^*(t_0^-) + \pi > 0$. Since the constraint $s_n(t) - s_{n+1}(t) \leq 0$ is not an explicit function of time, we have

$$\lambda_{s_n}^*(t_0^-) u_n^*(t_0^-) + \lambda_{s_{n+1}}^*(t_0^-) u_{n+1}^*(t_0^-) = \lambda_{s_n}^*(t_0^+) u_n^*(t_0^+) + \lambda_{s_{n+1}}^*(t_0^+) u_{n+1}^*(t_0^+) \quad (25)$$

On the other hand, $u_n^*(t_0^+) \leq 0$ and $u_{n+1}^*(t_0^+) \geq 0$, since agents n and $n+1$ must either come to rest or reverse their motion after making contact, hence $\lambda_{s_n}^*(t_0^+) u_n^*(t_0^+) + \lambda_{s_{n+1}}^*(t_0^+) u_{n+1}^*(t_0^+) \geq 0$. This violates (25), since $\lambda_{s_n}^*(t_0^-) u_n^*(t_0^-) + \lambda_{s_{n+1}}^*(t_0^-) u_{n+1}^*(t_0^-) < 0$. This contradiction implies that $s_n(t) - s_{n+1}(t) = 0$ cannot be active and we conclude that $s_n^*(t) \neq s_{n+1}^*(t)$ for $t \in [0, T]$, $n = 1, \dots, N-1$. Moreover, if one of the two agents is at rest when $s_n^*(t_0) = s_{n+1}^*(t_0)$, the same argument still holds since it is still true that $\lambda_{s_n}^*(t_0^-) u_n^*(t_0^-) + \lambda_{s_{n+1}}^*(t_0^-) u_{n+1}^*(t_0^-) < 0$. ■

Based on this analysis, the optimal control $u_n^*(t)$ depends entirely on the sign of $\lambda_{s_n}^*(t)$ and, in light of Propositions 3.1-3.3, the solution of the problem reduces to determining: (i) *switching points* in $[0, L]$ where an agent switches from $u_n^*(t) = \pm 1$ to either ∓ 1 or 0; or from $u_n^*(t) = 0$ to either ± 1 , and (ii) if an agent switches from $u_n^*(t) = \pm 1$ to 0, *waiting times* until the agent switches back to a speed $u_n^*(t) = \pm 1$. In other words, the full solution is characterized by two parameter vectors for each agent n : $\theta_n = [\theta_{n,1}, \dots, \theta_{n,\Gamma_n}]^T$ and $w_n = [w_{n,1}, \dots, w_{n,\Gamma_n}]^T$, where $\theta_{n,\xi} \in (0, L)$ denotes the ξ th location where agent n changes its speed from ± 1 to 0 and $w_{n,\xi} \geq 0$ denotes the time (which is possibly null) that agent n dwells on $\theta_{n,\xi}$. Note that Γ_n is generally not known a priori and depends on the time horizon T . In addition, we always assume that agent n reverses its velocity direction after leaving the switching point $\theta_{n,\xi}$ with respect to the one it had when reaching $\theta_{n,\xi}$. This seemingly excludes the possibility of an agent's control following a sequence 1, 0, 1 or $-1, 0, -1$. However, these two motion behaviors can be captured as two adjacent switching points approaching each other: when $|\theta_{n,\xi} - \theta_{n,\xi+1}| \rightarrow 0$, the agent control follows the sequence 1, 0, 1 or $-1, 0, -1$, and the waiting time associated with $u_n^*(t) = 0$ is $w_{n,\xi} + w_{n,\xi+1}$.

For simplicity, we will assume that $s_n(0) = 0$, so that it follows from Proposition 3.1 that $u_n^*(0) = 1$, $n = 1, \dots, N$. Therefore, $\theta_{n,1}$ corresponds to the optimal control switching from 1 to 0. Furthermore,

$\theta_{n,\xi}$ with ξ odd (even) always corresponds to $u_n^*(t)$ switching from 1 to 0 (-1 to 0.) Thus, we have the following constraints on the switching locations for all $\xi = 2, \dots, \Gamma_n$:

$$\begin{cases} \theta_{n,\xi} \leq \theta_{n,\xi-1}, & \text{if } \xi \text{ is even} \\ \theta_{n,\xi} \geq \theta_{n,\xi-1}, & \text{if } \xi \text{ is odd.} \end{cases} \quad (26)$$

It is now clear that the behavior of each agent under the optimal control policy is that of a *hybrid system* whose dynamics undergo switches when $u_n^*(t)$ changes from ± 1 to 0 and from 0 to ∓ 1 or when $R_i(t)$ reaches or leaves the boundary value $R_i = 0$. As a result, we are faced with a parametric optimization problem for a system with hybrid dynamics. This is a setting where one can apply the generalized theory of Infinitesimal Perturbation Analysis (IPA) in [15], [16] to conveniently obtain the gradient of the objective function J in (7) with respect to the vectors θ and w , and therefore, determine (generally, locally) optimal vectors θ^* and w^* through a gradient-based optimization approach. Note that this is done on line, i.e., the gradient is evaluated by observing a trajectory with given θ and w over $[0, T]$ based on which θ and w are adjusted until convergence is attained using standard gradient-based algorithms.

Remark 1. If the agent dynamics in (1) are replaced by a model such as $\dot{s}_n(t) = g_n(s_n) + b_n u_n(t)$, observe that (12) still holds. The difference lies in (10) which would involve a dependence on $\frac{dg_n(s_n)}{ds_n}$ and further complicate the associated two-point-boundary-value problem. However, since the optimal solution is also defined by a parameter vectors $\theta_n = [\theta_{n,1}, \dots, \theta_{n,\Gamma_n}]^T$ and $w_n = [w_{n,1}, \dots, w_{n,\Gamma_n}]^T$ for each agent n , we can still apply the IPA approach presented in the next section.

3.2 Infinitesimal Perturbation Analysis (IPA)

Our analysis thus far has shown that, on an optimal trajectory, the agent moves at full speed, dwells on a switching point (possibly for zero time) and never reaches either boundary point, i.e., $0 < s_n^*(t) < L$. Thus, the n th agent's movement can be parameterized through $\theta_n = [\theta_{n,1}, \dots, \theta_{n,\Gamma_n}]^T$ and $w_n = [w_{n,1}, \dots, w_{n,\Gamma_n}]^T$ where $\theta_{n,\xi}$ is the ξ th control switching point and $w_{n,\xi}$ is the waiting time for this agent at the ξ th switching point. Therefore, the solution of problem **P1** reduces to the determination of optimal parameter vectors θ_n^* and w_n^* , $n = 1, \dots, N$. As we pointed out, the agent's optimal behavior defines a hybrid system, and the switching locations translate to switching times between particular modes of this system. This is similar to switching-time optimization problems, e.g., [18], [19], [20], except that we can only control a subset of mode switching times. We make use of IPA in part to exploit robustness properties that the resulting gradients possess [21]; specifically, we will show that they do not depend on the uncertainty model parameters A_i , $i = 1, \dots, M$, and may therefore be used without any detailed knowledge of how uncertainty affects the mission space.

3.2.1 One agent solution with $a = 0$ and $b = L$

To maintain some notational simplicity, we begin with a single agent who can move on the entire mission space $[0, L]$ and will then provide the natural extension to multiple agents and a mission space limited to $[a, b] \subset [0, L]$. We present the associated hybrid automaton model for this single-agent system operating on an optimal trajectory. Our goal is to determine $\nabla J(\theta, w)$, the gradient of the objective function J in (7)

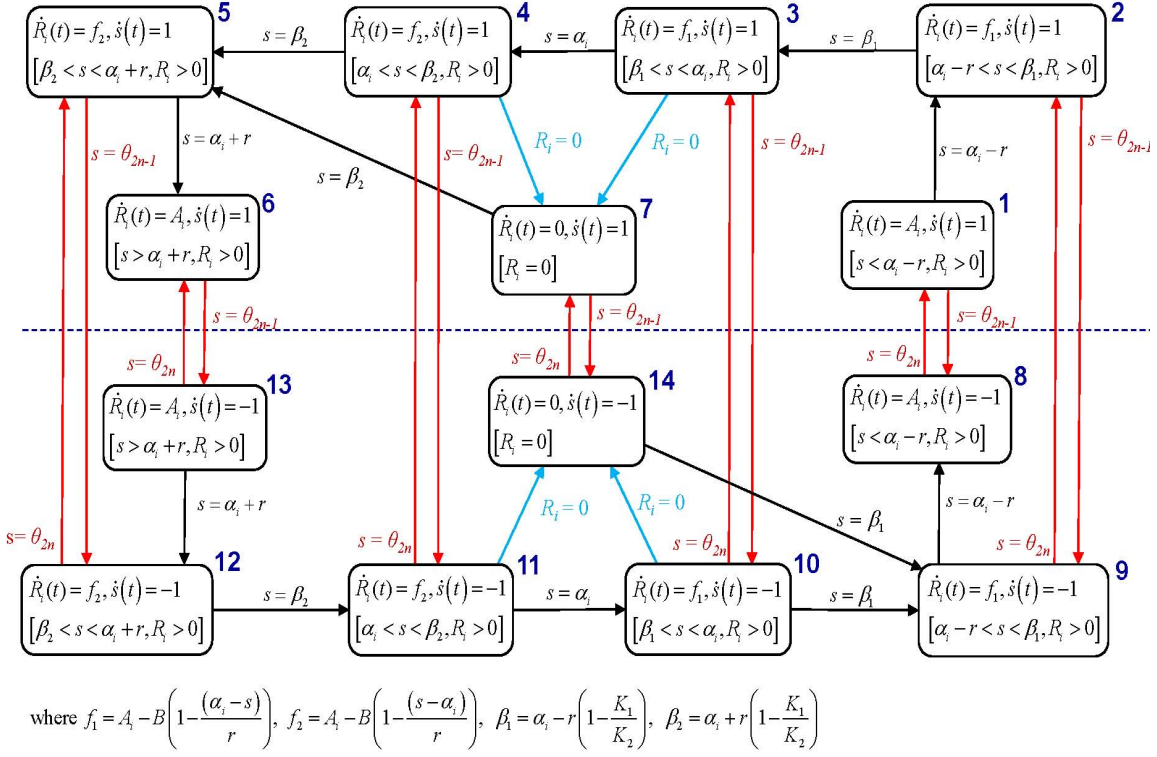


Figure 2: Hybrid automaton for each α_i . Red arrows represent events when the control switches between 1 and -1 . Blue arrows represent events when R_i becomes 0. Black arrows represent all other events.

with respect to θ and w , which can then be used in a gradient-based algorithm to obtain optimal parameter vectors θ_n^* and w_n^* , $n = 1, \dots, N$. We will apply IPA, which provides a formal way to obtain state and event time derivatives with respect to parameters of hybrid systems, from which we can subsequently obtaining $\nabla J(\theta, w)$.

Hybrid automaton model. We use a standard definition of a hybrid automaton (e.g., see [22]) as the formalism to model the system described above. Thus, let $q \in Q$ (a countable set) denote the discrete state (or mode) and $x \in X \subseteq \mathbb{R}^n$ denote the continuous state. Let $v \in Y$ (a countable set) denote a discrete control input and $u \in U \subseteq \mathbb{R}^m$ a continuous control input. Similarly, let $\delta \in \Delta$ (a countable set) denote a discrete disturbance input and $d \in D \subseteq \mathbb{R}^p$ a continuous disturbance input. The state evolution is determined by means of (i) a vector field $f : Q \times X \times U \times D \rightarrow X$, (ii) an invariant (or domain) set $Inv : Q \times Y \times \Delta \rightarrow 2^X$, (iii) a guard set $Guard : Q \times Q \times Y \times \Delta \rightarrow 2^X$, and (iv) a reset function $r : Q \times Q \times X \times Y \times \Delta \rightarrow X$. The system remains at a discrete state q as long as the continuous (time-driven) state x does not leave the set $Inv(q, v, \delta)$. If x reaches a set $Guard(q, q', v, \delta)$ for some $q' \in Q$, a discrete transition can take place. If this transition does take place, the state instantaneously resets to (q', x') where x' is determined by the reset map $r(q, q', x, v, \delta)$. Changes in v and δ are discrete events that either *enable* a transition from q to q' by making sure $x \in Guard(q, q', v, \delta)$ or *force* a transition out of q by making sure $x \notin Inv(q, v, \delta)$. We will classify all events that cause discrete state transitions in a manner that suits the purposes of IPA. Since our problem is set in a deterministic framework, δ and d will not be used.

We show in Fig. 2 a partial hybrid automaton model of the single-agent system where $a = 0$ and $b = L$. Since there is only one agent, we set $s(t) = s_1(t)$, $u(t) = u_1(t)$ and $\theta = \theta_1$ for simplicity. Due to the size of the overall model, Fig. 2 is limited to the behavior of the agent with respect to a single $\alpha_i, i \in \{1, \dots, M\}$ and ignores modes where the agent dwells on the switching points (these, however, are included in our extended analysis in Section 3.2.2.) The model consists of 14 discrete states (modes) and is symmetric in the sense that states 1 – 7 correspond to the agent operating with $u(t) = 1$, and states 8 – 14 correspond to the agent operating with $u(t) = -1$. States where $u(t) = 0$ are omitted since we do not include the waiting time parameter $w = w_1$ here. The events that cause state transitions can be placed in three categories: (i) The value of $R_i(t)$ becomes 0 and triggers a switch in the dynamics of (6). This can only happen when $R_i(t) > 0$ and $\dot{R}_i(t) = A_i - Bp_i(s(t)) < 0$ (e.g., in states 3 and 4), causing a transition to state 7 in which the invariant condition is $R_i(t) = 0$. (ii) The agent reaches a switching location, indicated by the guard condition $s(t) = \theta_\xi$ for any $\xi = 1, \dots, \Gamma$. In these cases, a transition results from a state z to $z + 7$ if $z = 1, \dots, 6$ and to $z - 7$ otherwise. (iii) The agent position reaches one of several critical values that affect the dynamics of $R_i(t)$ while $R_i(t) > 0$. Specifically, when $s(t) = \alpha_i - r$, the value of $p_i(s(t))$ becomes strictly positive and $\dot{R}_i(t) = A_i - Bp_i(s(t)) > 0$, as in the transition $1 \rightarrow 2$. Subsequently, when $s(t) = \alpha_i - r(1 - A_i/B)$, as in the transition $2 \rightarrow 3$, the value of $p_i(s(t))$ becomes sufficiently large to cause $\dot{R}_i(t) = A_i - Bp_i(s(t)) < 0$ so that a transition due to $R_i(t) = 0$ becomes feasible at this state. Similar transitions occur when $s(t) = \alpha_i$, $s(t) = \alpha_i + r(1 - A_i/B)$, and $s(t) = \alpha_i + r$. The latter results in state 6 where $\dot{R}_i(t) = A_i > 0$ and the only feasible event is $s(t) = \theta_\xi$, ξ odd, when a switch must occur and a transition to state 13 takes place (similarly for state 8).

IPA review. Before proceeding, we provide a brief review of the IPA framework for general stochastic hybrid systems as presented in [15]. The purpose of IPA is to study the behavior of a hybrid system state as a function of a parameter vector $\theta \in \Theta$ for a given compact, convex set $\Theta \subset \mathbb{R}^l$. Let $\{\tau_k(\theta)\}$, $k = 1, \dots, K$, denote the occurrence times of all events in the state trajectory. For convenience, we set $\tau_0 = 0$ and $\tau_{K+1} = T$. Over an interval $[\tau_k(\theta), \tau_{k+1}(\theta))$, the system is at some mode during which the time-driven state satisfies $\dot{x} = f_k(x, \theta, t)$. An event at τ_k is classified as (i) *Exogenous* if it causes a discrete state transition independent of θ and satisfies $\frac{d\tau_k}{d\theta} = 0$; (ii) *Endogenous*, if there exists a continuously differentiable function $g_k : \mathbb{R}^n \times \Theta \rightarrow \mathbb{R}$ such that $\tau_k = \min\{t > \tau_{k-1} : g_k(x(\theta, t), \theta) = 0\}$; and (iii) *Induced* if it is triggered by the occurrence of another event at time $\tau_m \leq \tau_k$. IPA specifies how changes in θ influence the state $x(\theta, t)$ and the event times $\tau_k(\theta)$ and, ultimately, how they influence interesting performance metrics which are generally expressed in terms of these variables.

Given $\theta = [\theta_1, \dots, \theta_\Gamma]^T$, we use the Jacobian matrix notation: $x'(t) \equiv \frac{\partial x(\theta, t)}{\partial \theta}$, $\tau'_k \equiv \frac{\partial \tau_k(\theta)}{\partial \theta}$, $k = 1, \dots, K$, for all state and event time derivatives. It is shown in [15] that $x'(t)$ satisfies:

$$\frac{d}{dt}x'(t) = \frac{\partial f_k(t)}{\partial x}x'(t) + \frac{\partial f_k(t)}{\partial \theta} \quad (27)$$

for $t \in [\tau_k, \tau_{k+1})$ with boundary condition:

$$x'(\tau_k^+) = x'(\tau_k^-) + [f_{k-1}(\tau_k^-) - f_k(\tau_k^+)] \tau'_k \quad (28)$$

for $k = 0, \dots, K$. In addition, in (28), the gradient vector for each τ_k is $\tau'_k = 0$ if the event at τ_k is exogenous and

$$\tau'_k = - \left[\frac{\partial g_k}{\partial x} f_k(\tau_k^-) \right]^{-1} \left(\frac{\partial g_k}{\partial \theta} + \frac{\partial g_k}{\partial x} x'(\tau_k^-) \right) \quad (29)$$

if the event at τ_k is endogenous (i.e., $g_k(x(\theta, \tau_k), \theta) = 0$) and defined as long as $\frac{\partial g_k}{\partial x} f_k(\tau_k^-) \neq 0$.

IPA equations. To clarify the presentation, we first note that $i = 1, \dots, M$ is used to index the points where uncertainty is measured; $\xi = 1, \dots, \Gamma$ indexes the components of the parameter vector; and $k = 1, \dots, K$ indexes event times. In order to apply the three fundamental IPA equations (27)-(29) to our system, we use the state vector $x(t) = [s(t), R_1(t), \dots, R_M(t)]^T$ and parameter vector $\theta = [\theta_1, \dots, \theta_\Gamma]^T$. We then identify all events that can occur in Fig. 2 and consider intervals $[\tau_k(\theta), \tau_{k+1}(\theta))$ over which the system is in one of the 14 states shown for each $i = 1, \dots, M$. Applying (27) to $s(t)$ with $f_k(t) = 1$ or -1 due to (1) and (12), the solution yields the gradient vector $\nabla s(t) = [\frac{\partial s}{\partial \theta_1}(t), \dots, \frac{\partial s}{\partial \theta_M}(t)]^T$, where

$$\frac{\partial s}{\partial \theta_\xi}(t) = \frac{\partial s}{\partial \theta_\xi}(\tau_k^+), \text{ for } t \in [\tau_k, \tau_{k+1}) \quad (30)$$

for all $k = 1, \dots, K$, i.e., for all states $z(t) \in \{1, \dots, 14\}$. Similarly, let $\nabla R_i(t) = [\frac{\partial R_i}{\partial \theta_1}(t), \dots, \frac{\partial R_i}{\partial \theta_M}(t)]^T$ for $i = 1, \dots, M$. We note from (6) that $f_k(t) = 0$ for states $z(t) \in Z_1 \equiv \{7, 14\}$; $f_k(t) = A_i$ for states $z(t) \in Z_2 \equiv \{1, 6, 8, 13\}$; and $f_k(t) = A_i - Bp_i(s(t))$ for all other states which we further classify into $Z_3 \equiv \{2, 3, 11, 12\}$ and $Z_4 \equiv \{4, 5, 9, 10\}$. Thus, solving (27) and using (30) gives:

$$\nabla R_i(t) = \nabla R_i(\tau_k^+) - \begin{cases} 0 & \text{if } z(t) \in Z_1 \cup Z_2 \\ B \left(\frac{\partial p_i(s)}{\partial s} \right) \nabla s(\tau_k^+) \cdot (t - \tau_k) & \text{otherwise} \end{cases}$$

where $\frac{\partial p_i(s)}{\partial s} = \pm \frac{1}{r}$ as evaluated from (4) depending on the sign of $\alpha_i - s(t)$ at each associated automaton state.

We now turn our attention to the determination of $\nabla s(\tau_k^+)$ and $\nabla R_i(\tau_k^+)$ which are needed to evaluate $\nabla R_i(t)$ above. To do so, we use (28), which involves the event time gradient vectors $\nabla \tau_k = [\frac{\partial \tau_k}{\partial \theta_1}, \dots, \frac{\partial \tau_k}{\partial \theta_\Gamma}]^T$ for $k = 1, \dots, K$ (the value of K depends on T .) Looking at Fig. 2, there are three readily distinguishable cases regarding the events that cause discrete state transitions:

Case 1: An event at time τ_k which is neither $R_i = 0$ nor $s = \theta_\xi$, for any $\xi = 1, \dots, \Gamma$. In this case, it is easy to see that the dynamics of both $s(t)$ and $R_i(t)$ are continuous, so that $f_{k-1}(\tau_k^-) = f_k(\tau_k^+)$ in (28) applied to $s(t)$ and $R_i(t)$, $i = 1, \dots, M$ gives:

$$\begin{cases} \nabla s(\tau_k^+) = \nabla s(\tau_k^-) \\ \nabla R_i(\tau_k^+) = \nabla R_i(\tau_k^-), \quad i = 1, \dots, M \end{cases} \quad (31)$$

Case 2: An event $R_i = 0$ at time τ_k . This corresponds to transitions $3 \rightarrow 7$, $4 \rightarrow 7$, $10 \rightarrow 14$ and $11 \rightarrow 14$ in Fig. 2 where the dynamics of $s(t)$ are still continuous, but the dynamics of $R_i(t)$ switch from $f_{k-1}(\tau_k^-) = A_i - Bp_i(s(\tau_k^-))$ to $f_k(\tau_k^+) = 0$. Thus, $\nabla s(\tau_k^-) = \nabla s(\tau_k^+)$, but we need to evaluate τ_k' to determine $\nabla R_i(\tau_k^+)$. Observing that this event is endogenous, (29) applies with $g_k = R_i = 0$ and we get

$$\frac{\partial \tau_k}{\partial \theta_\xi} = - \frac{\frac{\partial R_i}{\partial \theta_\xi}(\tau_k^-)}{A_i - Bp_i(s(\tau_k^-))}, \quad \xi = 1, \dots, \Gamma, \quad k = 1, \dots, K$$

It follows from (28) that

$$\frac{\partial R_i}{\partial \theta_\xi}(\tau_k^+) = \frac{\partial R_i}{\partial \theta_\xi}(\tau_k^-) - \frac{[A_i - Bp_i(s(\tau_k^-))] \frac{\partial R_i}{\partial \theta_\xi}(\tau_k^-)}{A_i - Bp_i(s(\tau_k^-))} = 0$$

Thus, whenever an event occurs at τ_k such that $R_i(\tau_k)$ becomes zero, $\frac{\partial R_i}{\partial \theta_\xi}(\tau_k^+)$ is always reset to 0 regardless of $\frac{\partial R_i}{\partial \theta_\xi}(\tau_k^-)$.

Case 3: An event at time τ_k due to a control sign change at $s = \theta_\xi$, $\xi = 1, \dots, \Gamma$. This corresponds to any transition between the upper and lower part of the hybrid automaton in Fig. 2. In this case, the dynamics of $R_i(t)$ are continuous and we have $\frac{\partial R_i}{\partial \theta_\xi}(\tau_k^+) = \frac{\partial R_i}{\partial \theta_\xi}(\tau_k^-)$ for all i, ξ, k . On the other hand, we have $\dot{s}(\tau_k^+) = u(\tau_k^+) = -u(\tau_k^-) = \pm 1$. Observing that any such event is endogenous, (29) applies with $g_k = s - \theta_\xi = 0$ for some $\xi = 1, \dots, \Gamma$ and we get

$$\frac{\partial \tau_k}{\partial \theta_\xi} = \frac{1 - \frac{\partial s}{\partial \theta_\xi}(\tau_k^-)}{u(\tau_k^-)} \quad (32)$$

Combining (32) with (28) and recalling that $u(\tau_k^+) = -u(\tau_k^-)$, we have

$$\frac{\partial s}{\partial \theta_\xi}(\tau_k^+) = \frac{\partial s}{\partial \theta_\xi}(\tau_k^-) + [u(\tau_k^-) - u(\tau_k^+)] \frac{1 - \frac{\partial s}{\partial \theta_\xi}(\tau_k^-)}{u(\tau_k^-)} = 2$$

where $\frac{\partial s}{\partial \theta_\xi}(\tau_k^-) = 0$ because $\frac{\partial s}{\partial \theta_\xi}(0) = 0 = \frac{\partial s}{\partial \theta_\xi}(t)$ for all $t \in [0, \tau_k)$, since the position of the agent cannot be affected by θ_ξ prior to this event.

In this case, we also need to consider the effect of perturbations to θ_j for $j < \xi$, i.e., prior to the current event time τ_k (clearly, for $j > \xi$, $\frac{\partial s}{\partial \theta_j}(\tau_k^+) = 0$ since the current position of the agent cannot be affected by future events.) Observe that since $g_k = s - \theta_\xi = 0$, we have $\frac{\partial g_k}{\partial \theta_j} = 0$ for $j \neq \xi$ and (29) gives

$$\frac{\partial \tau_k}{\partial \theta_j} = -\frac{\frac{\partial s}{\partial \theta_j}(\tau_k^-)}{u(\tau_k^-)}$$

so that using this in (28) we get:

$$\frac{\partial s}{\partial \theta_j}(\tau_k^+) = \frac{\partial s}{\partial \theta_j}(\tau_k^-) - \frac{[u(\tau_k^-) - u(\tau_k^+)] \frac{\partial s}{\partial \theta_j}(\tau_k^-)}{u(\tau_k^-)} = -\frac{\partial s}{\partial \theta_j}(\tau_k^-)$$

Combining the above results, the components of $\nabla s(\tau_k^+)$ where τ_k is the event time when $s(\tau_k) = \theta_\xi$ for some ξ , are given by

$$\frac{\partial s}{\partial \theta_j}(\tau_k^+) = \begin{cases} -\frac{\partial s}{\partial \theta_j}(\tau_k^-) & \text{if } j = 1, \dots, \xi - 1 \\ 2 & \text{if } j = \xi \\ 0 & \text{if } j > \xi \end{cases} \quad (33)$$

It follows from (30) and the analysis of all three cases above that $\frac{\partial s}{\partial \theta_\xi}(t)$ for all ξ is constant throughout an optimal trajectory except at transitions caused by control switching locations (*Case 3*). In particular, for the k th event corresponding to $s(\tau_k) = \theta_\xi$, $t \in [\tau_k, T]$, if $u(t) = 1$, then $\frac{\partial s}{\partial \theta_\xi}(t) = -2$ if ξ is odd, and $\frac{\partial s}{\partial \theta_\xi}(t) = 2$ if ξ is even; similarly, if $u(t) = -1$, then $\frac{\partial s}{\partial \theta_\xi}(t) = 2$ if ξ is odd and $\frac{\partial s}{\partial \theta_\xi}(t) = -2$ if ξ is even. In summary, we can write:

$$\frac{\partial s}{\partial \theta_\xi}(t) = \begin{cases} (-1)^\xi \cdot 2u(t) & t \geq \tau_k \\ 0 & t < \tau_k \end{cases}, \quad \xi = 1, \dots, \Gamma \quad (34)$$

Finally, we can combine (34) with our results for $\frac{\partial R_i}{\partial \theta_\xi}(t)$ in all three cases above. Letting $s(\tau_l) = \theta_\xi$, we obtain the following expression for $\frac{\partial R_i}{\partial \theta_\xi}(t)$ for all $k \geq l, t \in [\tau_k, \tau_{k+1})$:

$$\frac{\partial R_i}{\partial \theta_\xi}(t) = \frac{\partial R_i}{\partial \theta_\xi}(\tau_k^+) + \begin{cases} 0 & \text{if } z(t) \in Z_1 \cup Z_2 \\ (-1)^{\xi+1} \frac{2B}{r} u(\tau_k^+) \cdot (t - \tau_k) & \text{if } z(t) \in Z_3 \\ -(-1)^{\xi+1} \frac{2B}{r} u(\tau_k^+) \cdot (t - \tau_k) & \text{if } z(t) \in Z_4 \end{cases} \quad (35)$$

with boundary condition

$$\frac{\partial R_i}{\partial \theta_\xi}(\tau_k^+) = \begin{cases} 0 & \text{if } z(\tau_k^+) \in Z_1 \\ \frac{\partial R_i}{\partial \theta_\xi}(\tau_k^-) & \text{otherwise} \end{cases} \quad (36)$$

Objective Function Gradient Evaluation. Based on our analysis, the objective function (7) in problem **P1** can now be written as $J(\theta)$, a function of θ instead of $u(t)$ and we can rewrite it as

$$J(\theta) = \frac{1}{T} \sum_{i=1}^M \sum_{k=0}^K \int_{\tau_k(\theta)}^{\tau_{k+1}(\theta)} R_i(t, \theta) dt$$

where we have explicitly indicated the dependence on θ . We then obtain:

$$\nabla J(\theta) = \frac{1}{T} \sum_{i=1}^M \sum_{k=0}^K \left(\int_{\tau_k}^{\tau_{k+1}} \nabla R_i(t) dt + R_i(\tau_{k+1}) \nabla \tau_{k+1} - R_i(\tau_k) \nabla \tau_k \right)$$

Observing the cancelation of all terms of the form $R_i(\tau_k) \nabla \tau_k$ for all k (with $\tau_0 = 0, \tau_{K+1} = T$ fixed), we finally get

$$\nabla J(\theta) = \frac{1}{T} \sum_{i=1}^M \sum_{k=0}^K \int_{\tau_k(\theta)}^{\tau_{k+1}(\theta)} \nabla R_i(t) dt. \quad (37)$$

The evaluation of $\nabla J(\theta)$ therefore depends entirely on $\nabla R_i(t)$, which is obtained from (35)-(36) and the event times $\tau_k, k = 1, \dots, K$, given initial conditions $s(0) = 0, R_i(0)$ for $i = 1, \dots, M$ and $\nabla R_i(0) = 0$. Since $\nabla R_i(t)$ itself depends only on the event times $\tau_k, k = 1, \dots, K$, the gradient $\nabla J(\theta)$ is obtained by observing the switching times in a trajectory over $[0, T]$ characterized by the vector θ .

3.2.2 Multi agent solution where $a \geq 0$ and $b \leq L$

Next, we extend the results obtained in the previous section to the general multi-agent problem where we also allow $a \geq 0$ and $b \leq L$. Recall that we require $0 \leq a \leq r_n$ and $L - r_m \leq b \leq L$, for at least some $n, m = 1, \dots, N$ since, otherwise, controlling agent movement cannot affect $R_i(t)$ for all α_i located outside the sensing range of agents. We now include both parameter vectors $\theta_n = [\theta_{n,1}, \dots, \theta_{n,\Gamma_n}]^T$ and $w_n = [w_{n,1}, \dots, w_{n,\Gamma_n}]^T$ for each agent n and, for notational simplicity, concatenate them to construct $\theta = [\theta_1, \dots, \theta_N]^T$ and $w = [w_1, \dots, w_N]^T$. The solution of problem **P1** reduces to the determination of optimal parameter vectors θ^* and w^* and we will use IPA to evaluate $\nabla J(\theta, w) = [\frac{dJ(\theta, w)}{d\theta} \frac{dJ(\theta, w)}{dw}]^T$. Similar to (37), it is clear that this depends on $\nabla R_i(t) = [\frac{\partial R_i(t)}{\partial \theta} \frac{\partial R_i(t)}{\partial w}]^T$ and the event times $\tau_k, k = 1, \dots, K$, observed on a trajectory over $[0, T]$ with given θ and w .

IPA equations. We begin by recalling the dynamics of $R_i(t)$ in (6) which depend on the relative positions of all agents with respect to α_i and change at time instants τ_k such that either $R_i(\tau_k) = 0$ with $R_i(\tau_k^-) > 0$ or $A_i > BP_i(\mathbf{s}(\tau_k))$ with $R_i(\tau_k^-) = 0$. Moreover, using (1) and our analysis in Section 3.1, the dynamics of $s_n(t)$, $n = 1, \dots, N$, in an optimal trajectory can be expressed as follows. Define $\Theta_{n,\xi} = (\theta_{n,\xi-1}, \theta_{n,\xi})$ if ξ is odd and $\Theta_{n,\xi} = (\theta_{n,\xi}, \theta_{n,\xi-1})$ if ξ is even to be the ξ th interval between successive switching points for any $n = 1, \dots, N$, where $\theta_{n,0} = s_n(0)$. Then, for $\xi = 1, 2, \dots$,

$$\dot{s}_n(t) = \begin{cases} 1 & s_n(t) \in \Theta_{n,\xi}, \xi \text{ odd} \\ -1 & s_n(t) \in \Theta_{n,\xi}, \xi \text{ even} \\ 0 & \text{otherwise} \end{cases} \quad (38)$$

where transitions for $s_n(t)$ from ± 1 to ∓ 1 are incorporated by treating them as cases where $w_{n,\xi} = 0$, i.e., no dwelling at a switching point $\theta_{n,\xi}$ (in which case $\dot{s}_n(t) = 0$.) We can now concentrate on all events causing switches either in the dynamics of any $R_i(t)$, $i = 1, \dots, M$, or the dynamics of any $s_n(t)$, $n = 1, \dots, N$. From (28), any other event at some time τ_k in this hybrid system cannot modify the values of $\nabla R_i(t) = \left[\frac{\partial R_i(t)}{\partial \theta} \frac{\partial R_i(t)}{\partial w} \right]^T$ or $\nabla s_n(t) = \left[\frac{\partial s_n(t)}{\partial \theta_n} \frac{\partial s_n(t)}{\partial w_n} \right]^T$ at $t = \tau_k$.

First, applying (27) to $s_n(t)$ with $f_k(t) = 1, -1$ or 0 due to (38), the solution yields

$$\nabla s_n(t) = \nabla s_n(\tau_k^+), \text{ for } t \in [\tau_k, \tau_{k+1}) \quad (39)$$

for all $k = 1, \dots, K$, $n = 1, \dots, N$. Similarly, applying (27) to $R_i(t)$ and using (6) gives:

$$\frac{\partial R_i}{\partial \theta_{n,\xi}}(t) = \frac{\partial R_i}{\partial \theta_{n,\xi}}(\tau_k^+) - \begin{cases} 0 & \text{if } R_i(t) = 0, A_i < BP_i(\mathbf{s}(t)) \\ B \prod_{d \neq n} (1 - p_i(s_d(t))) \left(\frac{\partial p_i(s_n)}{\partial s_n} \right) \frac{\partial s_n(\tau_k^+)}{\partial \theta_{n,\xi}} \cdot (t - \tau_k) & \text{otherwise} \end{cases} \quad (40)$$

and

$$\frac{\partial R_i}{\partial w_{n,\xi}}(t) = \frac{\partial R_i}{\partial w_{n,\xi}}(\tau_k^+) - \begin{cases} 0 & \text{if } R_i(t) = 0, A_i < BP_i(\mathbf{s}(t)) \\ B \prod_{d \neq n} (1 - p_i(s_d(t))) \left(\frac{\partial p_i(s_n)}{\partial s_n} \right) \frac{\partial s_n(\tau_k^+)}{\partial w_{n,\xi}} \cdot (t - \tau_k) & \text{otherwise} \end{cases} \quad (41)$$

Thus, it remains to determine the components of $\nabla s_n(\tau_k^+)$ and $\nabla R_i(\tau_k^+)$ in (39)-(41) using (28). This involves the event time gradient vectors $\nabla \tau_k = \left[\frac{\partial \tau_k}{\partial \theta} \frac{\partial \tau_k}{\partial w} \right]^T$ for $k = 1, \dots, K$, which will be determined through (29). There are three possible cases regarding the events that cause switches in the dynamics of $R_i(t)$ or $s_n(t)$ as mentioned above:

Case 1: An event at time τ_k such that $\dot{R}_i(t)$ switches from $\dot{R}_i(t) = 0$ to $\dot{R}_i(t) = A_i - BP_i(\mathbf{s}(t))$. In this case, it is easy to see that the dynamics of both $s_n(t)$ and $R_i(t)$ are continuous, so that $f_{k-1}(\tau_k^-) = f_k(\tau_k^+)$ in (28) applied to $s_n(t)$ and $R_i(t)$, $i = 1, \dots, M$, $n = 1, \dots, N$, and we get

$$\nabla s_n(\tau_k^+) = \nabla s_n(\tau_k^-), \quad n = 1, \dots, N \quad (42)$$

$$\nabla R_i(\tau_k^+) = \nabla R_i(\tau_k^-), \quad i = 1, \dots, M \quad (43)$$

Case 2: An event at time τ_k such that $\dot{R}_i(t)$ switches from $\dot{R}_i(t) = A_i - BP_i(\mathbf{s}(t))$ to $\dot{R}_i(t) = 0$, i.e., $R_i(\tau_k)$ becomes zero. In this case, we need to first evaluate $\nabla \tau_k$ from (29) in order to determine $\nabla R_i(\tau_k^+)$ through

(28). Observing that this event is endogenous, (29) applies with $g_k = R_i = 0$ and we get

$$\nabla \tau_k = -\frac{\nabla R_i(\tau_k^-)}{A_i(\tau_k^-) - BP_i(\mathbf{s}(\tau_k^-))} \quad (44)$$

It follows from (28) that

$$\nabla R_i(\tau_k^+) = \nabla R_i(\tau_k^-) - \frac{[A_i(\tau_k^-) - BP_i(\mathbf{s}(t))]\nabla R_i(\tau_k^-)}{A_i(\tau_k^-) - BP_i(\tau_k^-)} = 0 \quad (45)$$

Thus, $\nabla R_i(\tau_k^+)$ is always reset to 0 regardless of $\nabla R_i(\tau_k^-)$. In addition, (42) holds, since the the dynamics of $s_n(t)$ are continuous at time τ_k .

Case 3: An event at time τ_k such that the dynamics of $s_n(t)$ switch from ± 1 to 0, or from 0 to ± 1 . Clearly, (43) holds since the the dynamics of $R_i(t)$ are continuous at this time. However, determining $\nabla s_n(\tau_k^+)$ is more elaborate and requires us to consider its components separately, first $\frac{\partial s_n(\tau_k^+)}{\partial \theta_n}$ and then $\frac{\partial s_n(\tau_k^+)}{\partial w_n}$.

Case 3.1: Evaluation of $\frac{\partial s_n(\tau_k^+)}{\partial \theta_n}$.

Case 3.1.1: An event at time τ_k such that the dynamics of $s_n(t)$ in (38) switch from ± 1 to 0. This is an endogenous event and (29) applies with $g_k = s_n - \theta_{n,\xi} = 0$ for some $\xi = 1, \dots, \Gamma_n$ and we have:

$$\frac{\partial \tau_k}{\partial \theta_{n,\xi}} = \frac{1 - \frac{\partial s_n}{\partial \theta_{n,\xi}}(\tau_k^-)}{u_n(\tau_k^-)} \quad (46)$$

and (28) yields

$$\frac{\partial s_n}{\partial \theta_{n,\xi}}(\tau_k^+) = \frac{\partial s_n}{\partial \theta_{n,\xi}}(\tau_k^-) + [u_n(\tau_k^-) - 0] \frac{1 - \frac{\partial s_n}{\partial \theta_{n,\xi}}(\tau_k^-)}{u_n(\tau_k^-)} = 1 \quad (47)$$

As in Case 3 of Section 3.2.1, we also need to consider the effect of perturbations to θ_j for $j < \xi$, i.e., prior to the current event time τ_k (clearly, for $j > \xi$, $\frac{\partial s_n}{\partial \theta_j}(\tau_k^+) = 0$ since the current position of the agent cannot be affected by future events.) Observe that $\frac{\partial g_k}{\partial \theta_j} = 0$, therefore, (29) becomes

$$\frac{\partial \tau_k}{\partial \theta_{n,j}} = -\frac{\frac{\partial s_n}{\partial \theta_{n,j}}(\tau_k^-)}{u_n(\tau_k^-)} \quad (48)$$

and using this in (28) gives:

$$\frac{\partial s_n}{\partial \theta_{n,j}}(\tau_k^+) = \frac{\partial s_n}{\partial \theta_{n,j}}(\tau_k^-) - \frac{[u_n(\tau_k^-) - 0] \frac{\partial s_n}{\partial \theta_{n,j}}(\tau_k^-)}{u_n(\tau_k^-)} = 0 \quad (49)$$

Thus, combining the above results, when $s_q(\tau_k) = \theta_{q,\xi}$ for some ξ and the agent switches from ± 1 to 0, we have

$$\frac{\partial s_n}{\partial \theta_{n,j}}(\tau_k^+) = \begin{cases} 0, & \text{if } j \neq \xi \\ 1, & \text{if } j = \xi \end{cases} \quad (50)$$

Case 3.1.2: An event at time τ_k such that the dynamics of $s_n(t)$ in (38) switch from 0 to ± 1 . This is an induced event since it is triggered by the occurrence of some other endogenous event when the agent switches from ± 1 to 0 (see *Case 3.1.1* above.) Suppose the agent starts from an initial position $s_n(0) = a$ with $u_n(0) = 1$ and τ_k is the time the agent switches from the 0 to ± 1 at the switching point $\theta_{n,\xi}$. If $\theta_{n,\xi}$ is such that $u_n(\tau_k^+) = 1$, then ξ is even and τ_k can be calculated as follows:

$$\begin{aligned}\tau_k &= (\theta_{n,1} - a) + w_{n,1} + (\theta_{n,1} - \theta_{n,2}) + w_{n,2} + \dots + (\theta_{n,\xi-1} - \theta_{n,\xi}) + w_{n,\xi} \\ &= 2 \left(\sum_{v=1, v \text{ odd}}^{\xi-1} \theta_{n,v} - \sum_{v=2, v \text{ even}}^{\xi-2} \theta_{n,v} \right) + \sum_{v=1}^{\xi} w_{n,v} - \theta_{n,\xi}\end{aligned}\quad (51)$$

Similarly, if $\theta_{n,\xi}$ is the switching point such that $u_n(\tau_k^+) = -1$, then ξ is odd and we get:

$$\tau_k = 2 \left(\sum_{v=1, v \text{ odd}}^{\xi-2} \theta_{n,v} - \sum_{v=2, v \text{ even}}^{\xi-1} \theta_{n,v} \right) + \sum_{v=1}^{\xi} w_{n,v} + \theta_{n,\xi}\quad (52)$$

We can then directly obtain $\frac{\partial \tau_k}{\partial \theta_{n,\xi}}$ as

$$\frac{\partial \tau_k}{\partial \theta_{n,\xi}} = -\text{sgn}(u(\tau_k^+))\quad (53)$$

Using (53) in (28) gives:

$$\frac{\partial s_n}{\partial \theta_{n,\xi}}(\tau_k^+) = \frac{\partial s_n}{\partial \theta_{n,\xi}}(\tau_k^-) + [0 - u(\tau_k^+)] \cdot [-\text{sgn}(u(\tau_k^+))] = \frac{\partial s_n}{\partial \theta_{n,\xi}}(\tau_k^-) + 1\quad (54)$$

Once again, we need to consider the effect of perturbations to θ_j for $j < \xi$, i.e., prior to the current event time τ_k (clearly, for $j > \xi$, $\frac{\partial s_n}{\partial \theta_j}(\tau_k^+) = 0$.) In this case, from (51)-(52), we have

$$\begin{cases} \frac{\partial \tau_k}{\partial \theta_{n,j}} = 2, & \text{if } j \text{ odd} \\ \frac{\partial \tau_k}{\partial \theta_{n,j}} = -2, & \text{if } j \text{ even} \end{cases}\quad (55)$$

and it follows from (28) that for $j < \xi$:

$$\frac{\partial s_n}{\partial \theta_{n,j}}(\tau_k^+) = \begin{cases} \frac{\partial s_n}{\partial \theta_{n,j}}(\tau_k^-) + 2, & \text{if } u_n(\tau_k^+) = 1, j \text{ even, or } u_n(\tau_k^+) = -1, j \text{ odd} \\ \frac{\partial s_n}{\partial \theta_{n,j}}(\tau_k^-) - 2, & \text{if } u_n(\tau_k^+) = 1, j \text{ odd, or } u_n(\tau_k^+) = -1, j \text{ even} \end{cases}\quad (56)$$

Case 3.2: Evaluation of $\frac{\partial s_n(\tau_k^+)}{\partial w_n}$.

Case 3.2.1: An event at time τ_k such that the dynamics of $s_n(t)$ in (38) switch from ± 1 to 0. This is an endogenous event and (29) applies with $g_k = s_n - \theta_{n,\xi} = 0$ for some $\xi = 1, \dots, \Gamma_n$. Then, for any $j \leq \xi$, we have:

$$\frac{\partial \tau_k}{\partial w_{n,j}} = \frac{-\frac{\partial s_n}{\partial w_{n,j}}(\tau_k^-)}{u_n(\tau_k^-)}\quad (57)$$

Combining (57) with (28) and since $u_n(\tau_k^-) = \pm 1$, we have

$$\frac{\partial s_n}{\partial w_{n,j}}(\tau_k^+) = \frac{\partial s_n}{\partial w_{n,j}}(\tau_k^-) + [u_n(\tau_k^-) - 0] \frac{-\frac{\partial s_n}{\partial w_{n,j}}(\tau_k^-)}{u_n(\tau_k^-)} = 0 \quad (58)$$

Case 3.2.2: An event at time τ_k such that the dynamics of $s_n(t)$ in (38) switch from 0 to ± 1 . As in *Case 3.1.2*, τ_k is given by (51) or (52), depending on the sign of $u_q(\tau_k^+)$. Thus, we have $\frac{\partial \tau_k}{\partial w_{n,j}} = 1$, for $j \leq \xi$.

Using this result in (28) and observing that $\frac{\partial s_n}{\partial w_{n,j}}(\tau_k^-) = 0$ from (58), we have

$$\frac{\partial s_n}{\partial w_{n,j}}(\tau_k^+) = \frac{\partial s_n}{\partial w_{n,j}}(\tau_k^-) + [0 - u_n(\tau_k^+)] \cdot 1 = -u_n(\tau_k^+), \text{ for } j \leq \xi \quad (59)$$

Combining the above results, we have for *Case 3.2*:

$$\frac{\partial s_n}{\partial w_{n,j}}(\tau_k^+) = \begin{cases} 0, & \text{if } u_n(\tau_k^-) = \pm 1, u_n(\tau_k^+) = 0 \\ \mp 1, & \text{if } u_n(\tau_k^-) = 0, u_n(\tau_k^+) = \pm 1 \end{cases} \quad (60)$$

Finally, note that $\frac{\partial s_n}{\partial w_{n,\xi}}(t) = 0$ for $t \in [0, \tau_k)$, since the position of the agent n cannot be affected by $w_{n,\xi}$ prior to such an event.

Objective Function Gradient Evaluation. Proceeding as in the evaluation of $\nabla J(\theta)$ in Section 3.2.1, we are now interested in minimizing the objective function $J(\theta, w)$ in (7) with respect to θ and w and we can obtain $\nabla J(\theta, w) = [\frac{dJ(\theta, w)}{d\theta} \frac{dJ(\theta, w)}{dw}]^T$ as

$$\nabla J(\theta, w) = \frac{1}{T} \sum_{i=1}^M \sum_{k=0}^K \int_{\tau_k(\theta, w)}^{\tau_{k+1}(\theta, w)} \nabla R_i(t) dt$$

This depends entirely on $\nabla R_i(t)$, which is obtained from (40) and (41) and the event times τ_k , $k = 1, \dots, K$, given initial conditions $s_n(0) = a$ for $n = 1, \dots, N$, and $R_i(0)$ for $i = 1, \dots, M$. In (40), $\frac{\partial R_i}{\partial \theta_{n,\xi}}(\tau_k^+)$ is obtained through (43) and (45), whereas $\frac{\partial s_n(\tau_k^+)}{\partial \theta_{n,\xi}}$ is obtained through (39), (42), (50), and (56). In (41), $\frac{\partial R_i}{\partial w_{n,\xi}}(\tau_k^+)$ is again obtained through (43) and (45), whereas $\frac{\partial s_n(\tau_k^+)}{\partial w_{n,\xi}}$ is obtained through (42), and (60).

Remark 2. Observe that the evaluation of $\nabla R_i(t)$, hence $\nabla J(\theta, w)$, is independent of A_i , $i = 1, \dots, M$, i.e., the values in our uncertainty model. In fact, the dependence of $\nabla R_i(t)$ on A_i , $i = 1, \dots, M$, manifests itself through the event times τ_k , $k = 1, \dots, K$, that do affect this evaluation, but they, unlike A_i which may be unknown, are directly observable during the gradient evaluation process. Thus, the IPA approach possesses an inherent *robustness* property: there is no need to explicitly model how uncertainty affects $R_i(t)$ in (6). Consequently, we may treat A_i as unknown without affecting the solution approach (the values of $\nabla R_i(t)$ are obviously affected). We may also allow this uncertainty to be modeled through random processes $\{A_i(t)\}$, $i = 1, \dots, M$; in this case, however, the result of Proposition 3.3 no longer applies without some conditions on the statistical characteristics of $\{A_i(t)\}$ and the resulting $\nabla J(\theta, w)$ is an estimate of a stochastic gradient.)

3.3 Objective Function Optimization

We now seek to obtain θ^* and w^* minimizing $J(\theta, w)$ through a standard gradient-based optimization scheme of the form

$$[\theta^{l+1} w^{l+1}]^T = [\theta^l w^l]^T - [\eta_\theta \ \eta_w] \tilde{\nabla} J(\theta^l, w^l) \quad (61)$$

where $\{\eta_\theta^l\}, \{\eta_w^l\}$ are appropriate step size sequences and $\tilde{\nabla} J(\theta^l, w^l)$ is the projection of the gradient $\nabla J(\theta^l, w^l)$ onto the feasible set (the set of θ^{l+1} satisfying the constraint (26), $a \leq \theta^{l+1} \leq b$, and $w^l \geq 0$). The optimization scheme terminates when $|\tilde{\nabla} J(\theta, w)| < \varepsilon$ (for a fixed threshold ε) for some θ and w . Our IPA-based algorithm to obtain θ^* and w^* minimizing $J(\theta, w)$ is summarized in Algorithm 1 where we have adopted the Armijo method in step-size selection (see [23]) for $\{[\eta_\theta^l \ \eta_w^l]\}$.

One of the unusual features in (61) is the fact that the dimension Γ_n^* of θ_n^* and w_n^* is a priori unknown (it depends on T). Thus, the algorithm must implicitly determine this value along with θ_n^* and w_n^* . One can search over feasible values of $\Gamma_n \in \{1, 2, \dots\}$ by starting either with a lower bound $\Gamma_n = 1$ or an upper bound to be found. The latter approach results in much faster execution and is followed in Algorithm 1. An upper bound is determined by observing that $\theta_{n,\xi}$ is the switching point where agent n changes speed from 1 to 0 for ξ odd and from -1 to 0 for ξ even. By setting these two groups of switching points so that their distance is sufficiently small and waiting times $w_n = \mathbf{0}$ for each agent, we determine an approximate upper bound for Γ_n as follows. First, we divide the feasible space $[a, b]$ evenly into N intervals: $[a + \frac{n-1}{N}(b-a), a + \frac{n}{N}(b-a)]$, $n = 1, \dots, N$. Define $D_n = a + \frac{2n-1}{2N}(b-a)$ to be the geometric center of each interval and set

$$\begin{cases} \theta_{n,\xi} = D_n - \sigma & \text{if } \xi \text{ even} \\ \theta_{n,\xi} = D_n + \sigma & \text{if } \xi \text{ odd} \end{cases} \quad (62)$$

so that the distance between switching points $\theta_{n,\xi}$ for ξ odd and even is 2σ , where $\sigma > 0$ is an arbitrarily small number, $n = 1, \dots, N$. In addition, set $w_n = \mathbf{0}$. Then, T must satisfy

$$\theta_{n,1} - s_n(0) + 2\sigma(\Gamma_n - 1) \leq T \leq \theta_{n,1} - s_n(0) + 2\sigma\Gamma_n \quad (63)$$

$n = 1, \dots, N$, where Γ_n is the number of switching points agent n can reach during $(0, T]$, given $\theta_{n,\xi}$ are defined in (62). From (63) and noting that Γ_n is an integer, we have

$$\Gamma_n = \left\lceil \frac{1}{2\sigma} [T - \theta_{n,1} + s_n(0)] \right\rceil \quad (64)$$

where $\lceil \cdot \rceil$ is the ceiling function. Clearly, reducing σ increases the initial number of switching points Γ_n assigned to agent n and $\Gamma_n \rightarrow \infty$ as $\sigma \rightarrow 0$. Therefore, σ is selected sufficiently small while ensuring that the algorithm can be executed sufficiently fast.

As Algorithm 1 repeats steps 3-6, $w_{n,\xi} \geq 0$ and distances between $\theta_{n,\xi}$ for ξ odd and even generally increase, so that the number of switching points agent n can actually reach within T decreases. In other words, as long as σ is sufficiently small (hence, Γ_n is sufficiently large), when the algorithm converges to a local minimum and stops, there exists $\zeta_n < \Gamma_n$, such that θ_{n,ζ_n} is the last switching point agent n can reach within $(0, T]$, $n = 1, \dots, N$. Observe that there generally exist ξ such that $\zeta_n < \xi \leq \Gamma_n$ which correspond to points $\theta_{n,\xi}$ that agent n cannot reach within $(0, T]$; the associated derivatives of the cost with respect to such $\theta_{n,\xi}$ are 0, since perturbations to these $\theta_{n,\xi}$ will not affect $s_n(t)$, $t \in (0, T]$ and thus the cost $J(\theta, w)$. When $|\tilde{\nabla} J(\theta, w)| < \varepsilon$, we achieve a local minimum and stop, at which point the dimension of θ_n^* and w_n^* is ζ_n .

Algorithm 1 : IPA-based optimization algorithm to find θ^* and w^*

- 1: Pick $\sigma > 0$ and $\varepsilon > 0$.
 - 2: Define $D_n = a + \frac{2n-1}{2N}(b-a)$, $n = 1, \dots, N$, and set $\begin{cases} \theta_{n,\xi} = D_n - \sigma & \text{if } \xi \text{ even} \\ \theta_{n,\xi} = D_n + \sigma & \text{if } \xi \text{ odd} \end{cases}$.
Set $w = [w_1, \dots, w_N] = 0.$, where $w_n = [w_{n,1}, \dots, w_{n,\xi_n}]$ and $\Gamma_n = \lceil \frac{1}{2\sigma} [T - \theta_{n,1} + s_n(0)] \rceil$
 - 3: **repeat**
 - 4: Compute $s_n(t)$, $t \in [0, T]$ using $s_n(0)$, (12), θ and w for $n = 1, \dots, N$
 - 5: Compute $\tilde{\nabla}J(\theta, w)$ and update θ, w through (61)
 - 6: **until** $|\tilde{\nabla}J(\theta, w)| < \varepsilon$
 - 7: Set $\theta_n^* = [\theta_{n,1}^*, \dots, \theta_{n,\xi_n}^*]$ and $w_n^* = [w_{n,1}^*, \dots, w_{n,\xi_n}^*]$, where ξ_n is the index of θ_{n,ξ_n} , which is the last switching point agent n can reach within $(0, T]$, $n = 1, \dots, N$
-

4 Numerical Results

In this section we present some examples of persistent monitoring problems in which agent trajectories are determined using Algorithm 1. The first four are one-agent examples with $L = 20$, $M = 21$, $\alpha_1 = 0$, $\alpha_M = 20$, and the remaining sampling points are evenly spaced over $[0, 20]$. The sensing range in (4) is set to $r = 4$, the initial values of the uncertainty functions in (6) are $R_i(0) = 4$ for all i , and the time horizon is $T = 400$. In Fig. 3(a) we show results where the agent is allowed to move over the entire space $[0, 20]$ and the uncertainty model is selected so that $B = 3$ and $A_i = 0.1$ for all $i = 1, \dots, 20$, whereas in Fig. 3(b) the feasible space is limited to $[a, b]$ with $a = r = 4$ and $b = L - r = 16$. The top plot in each example shows the optimal trajectory $s^*(t)$ obtained, while the bottom shows the cost $J(\theta^l, w^l)$ as a function of iteration number. In Fig. 4, the trajectories in Fig. 3(a),(b) are magnified for the interval $t \in [0, 75]$ to emphasize the presence of strictly positive waiting times at the switching points. In addition, maximum, minimum and mean values for the uncertainty function of each sampling point in these two cases are shown in Fig. 5. Observe that when $a = r$ and $b = L - r$, an instability arises at the last two sampling points of both ends of the mission space; this is expected since the agent's sensing range can only marginally reach the two end points from $a = 4$ and $b = 16$.

In Fig. 3(c) we show results for a case similar to Fig. 3(a) except that the values of A_i are selected so that $A_0 = A_{20} = 0.5$, while $A_i = 0.1$, $i = 1, \dots, 19$. We should point out that even though it seems that the trajectory includes switching points at the two end points, this is not the case: the switching points are very close but not equal to these end points, consistent with Proposition 3.1. In Fig. 3(d), on the other hand, the values of A_i are allowed to be random, thus dealing with a persistent monitoring problem in a stochastic mission space. In particular, each A_i is treated as a piecewise constant random process $\{A_i(t)\}$ such that $A_i(t)$ takes on a fixed value uniformly distributed over $(0.075, 0.125)$ for an exponentially distributed time interval with mean 10 before switching to a new value. Note that the behavior of the system in this case is very similar to Fig. 3(a) where $A_i = 0.1$ for all $i = 1, \dots, 20$ without any change in the way in which $\nabla J(\theta^l, w^l)$ is evaluated in executing (61). As already pointed out, this exploits a robustness property of IPA which makes it independent of the values of A_i . In general, however, when $A_i(t)$ is not time-invariant, Proposition 3.3 may no longer apply, since an extra term $\sum_i \dot{A}_i(t)$ would be present in (22). In such a case, $u_n^*(t)$ may be nonzero when $\lambda_n^*(t) = 0$ and the determination of an optimal trajectory through switching points and waiting times alone may no longer be possible. In the case of 3(d), $A_i(t)$ changes sufficiently slowly to maintain the validity of Proposition 3.3 over relatively

long time intervals, under the assumption that w.p. 1 no event time coincides with the jump times in any $\{A_i(t)\}$.

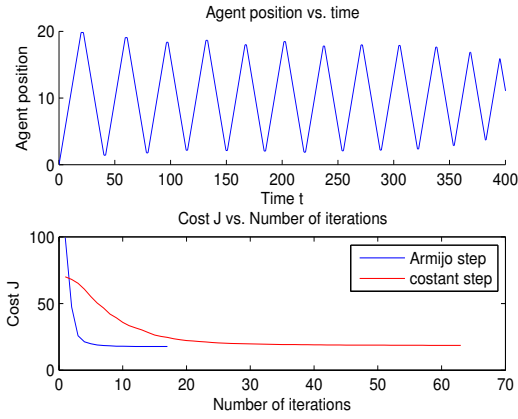
In all cases, we initialize the algorithm with $\sigma = 5$ and $\varepsilon = 2 \times 10^{-10}$. The algorithm running times are approximately 10 sec using Armijo step-sizes. Note that although the number of iterations for the examples shown may substantially vary, the actual algorithm running times do not. This is simply because the Armijo step-size method may involve several trials per iteration to adjust the step-size in order to achieve an adequate decrease in cost. In Fig. 3(a),(d), red line shows J vs. number of iterations using constant step size and they almost converges to the same optimal value. Non-smoothness in Fig. 3(d) comes from the fact that it is a stochastic system. Note that in all cases the initial cost is significantly reduced indicating the importance of optimally selecting the values of the switching points and associated waiting times (if any).

Figure 6 shows two two-agent examples with $L = 40$, $M = 41$ and evenly spaced sampling points over $[0, L]$, $A_i = 0.01$, $B = 3$, $r = 4$, $R_i(0) = 4$ for all i and $T = 400$. In Fig. 6(a) the agents are allowed to move over the whole mission space $[0, L]$, while in Fig. 6(b) they are only allowed to move over $[a, b]$ where $a = r$ and $b = L - r$. We initialize the algorithm with the same σ and ε as before. The algorithm running time is approximately 15 sec using Armijo step-sizes, and we observe once again significant reductions in cost.

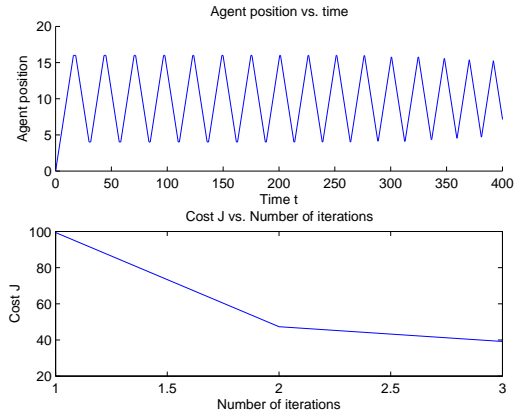
5 Conclusion

References

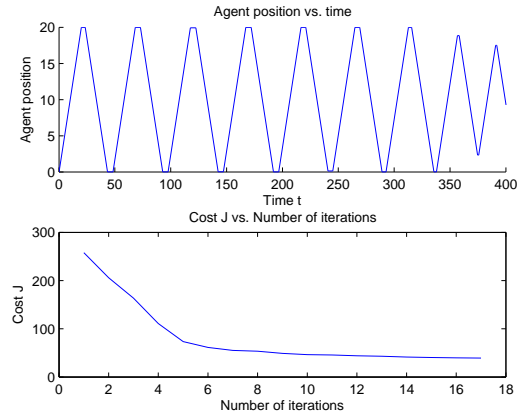
- [1] I. Rekleitis, V. Lee-Shue, A. New, and H. Choset, "Limited communication, multi-robot team based coverage," in *Robotics and Automation, 2004. Proceedings. ICRA'04. 2004 IEEE International Conference on*, vol. 4. IEEE, 2004, pp. 3462–3468.
- [2] J. Cortes, S. Martinez, T. Karatas, and F. Bullo, "Coverage control for mobile sensing networks," *Robotics and Automation, IEEE Transactions on*, vol. 20, no. 2, pp. 243–255, 2004.
- [3] W. Li and C. Cassandras, "A cooperative receding horizon controller for multivehicle uncertain environments," *IEEE Transactions on Automatic Control*, vol. 51, no. 2, pp. 242–257, 2006.
- [4] A. Girard, A. Howell, and J. Hedrick, "Border patrol and surveillance missions using multiple unmanned air vehicles," in *43rd IEEE Conference on Decision and Control*, vol. 1. IEEE, 2005, pp. 620–625.
- [5] B. Grocholsky, J. Keller, V. Kumar, and G. Pappas, "Cooperative air and ground surveillance," *IEEE Robotics & Automation Magazine*, vol. 13, no. 3, pp. 16–25, 2006.
- [6] S. Smith, M. Schwager, and D. Rus, "Persistent robotic tasks: Monitoring and sweeping in changing environments," *IEEE Transactions on Robotics*, 2012, to appear.
- [7] D. Paley, F. Zhang, and N. Leonard, "Cooperative control for ocean sampling: The glider coordinated control system," *IEEE Transactions on Control Systems Technology*, vol. 16, no. 4, pp. 735–744, 2008.



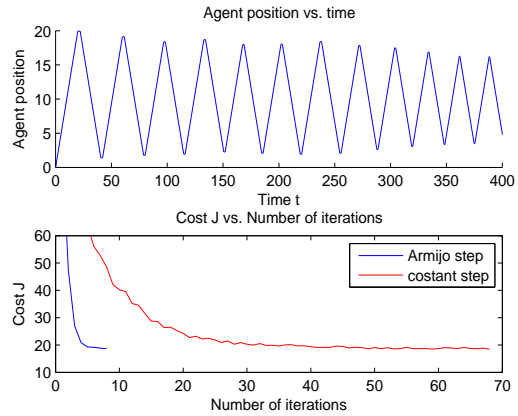
(a) $a = 0, b = 20. A_i = 0.1, i = 1, \dots, 20. J^* = 17.77.$



(b) $a = 4, b = 16. A_i = 0.1, i = 1, \dots, 20. J^* = 39.14.$

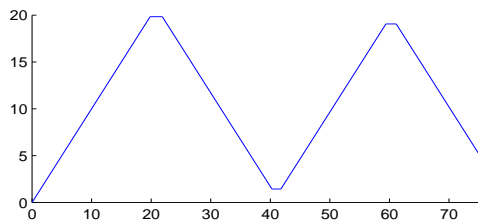


(c) $a = 0, b = 20. A_0 = A_{20} = 0.5, A_i = 0.1, i = 1, \dots, 19. J^* = 39.30.$

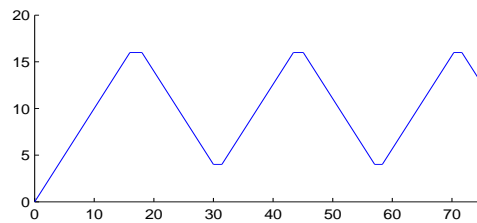


(d) $a = 0, b = 20. A_i(\Delta t_i) \sim U(0.075, 0.125), \Delta t_i \sim 0.1e^{-0.1t}. J^* = 17.54.$

Figure 3: One agent example. $L = 20, T = 400$. For each example, top plot: optimal trajectory; bottom plot: J versus iterations.



(a) $a = 0, b = 20.$



(b) $a = 4, b = 16.$

Figure 4: Magnified trajectory for sub-figure (a) and (b) in Fig. 3, $t \in [0, 75]$.

	Max	Min	Mean
1	5.7375	0	1.7149
2	3.1840	0	1.3001
3	2.9840	0	1.0963
4	2.7840	0	0.9456
5	4.0067	0	0.8104
6	4.1067	0	0.6899
7	4.2067	0	0.5847
8	4.3067	0	0.5044
9	4.4067	0	0.4470
10	4.5067	0	0.4129
11	4.6067	0	0.4035
12	4.7067	0	0.4192
13	4.8067	0	0.4603
14	4.9067	0	0.5267
15	5.0067	0	0.6170
16	5.1067	0	0.7316
17	5.2067	0	0.8642
18	5.3067	0	1.0123
19	5.4067	0	1.1725
20	5.5067	0	1.3613
21	5.6067	0	1.6992

(a) $a = 0, b = 20$.

	Max	Min	Mean
1	39.6067	0	19.6167
2	22.4569	0	9.4710
3	2.8878	0	1.0591
4	2.0130	0	0.8189
5	4.0067	0	0.6729
6	4.1067	0	0.5446
7	4.2067	0	0.4311
8	4.3067	0	0.3350
9	4.4067	0	0.2589
10	4.5067	0	0.2158
11	4.6067	0	0.2078
12	4.7067	0	0.2349
13	4.8067	0	0.2971
14	4.9067	0	0.3919
15	5.0067	0	0.5067
16	5.1067	0	0.6380
17	5.2067	0	0.7859
18	5.3067	0	0.9506
19	5.4067	0	1.2171
20	25.6269	3.6605	12.5340
21	44.0000	5.5990	24.0000

(b) $a = 4, b = 16$.

Figure 5: Max, min and mean uncertainty value for each sampling point.

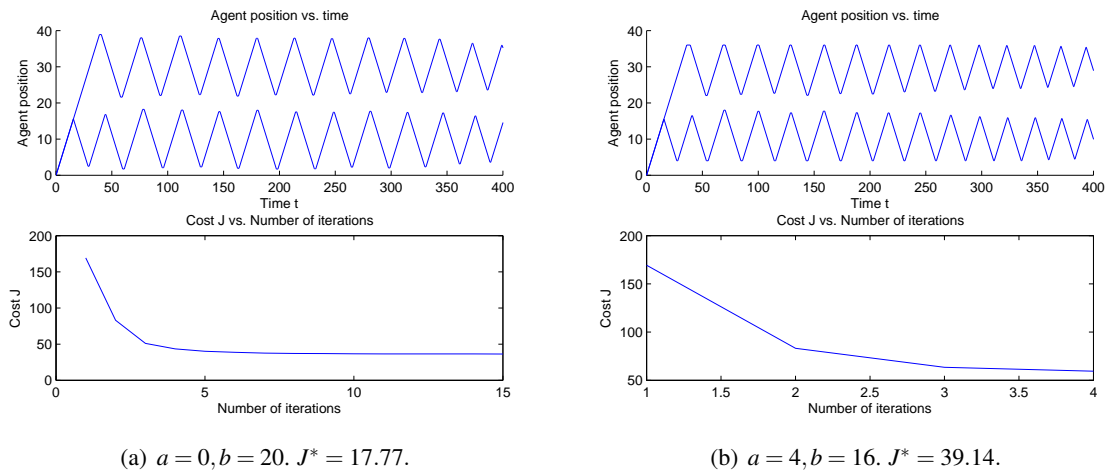


Figure 6: Two agent example. $L = 40, T = 400$. Top plot: optimal trajectory. Bottom plot: J versus iterations.

- [8] D. Bertsimas and G. Van Ryzin, “Stochastic and dynamic vehicle routing in the Euclidean plane with multiple capacitated vehicles,” *Operations Research*, pp. 60–76, 1993.
- [9] R. Cooper, *Introduction to queuing theory*. Edward Arnold, 1981.
- [10] G. Sun, C. Cassandras, Y. Wardi, C. Panayiotou, and G. Riley, “Perturbation analysis and optimization of stochastic flow networks,” *Automatic Control, IEEE Transactions on*, vol. 49, no. 12, pp. 2143–2159, 2004.
- [11] N. Nigam and I. Kroo, “Persistent surveillance using multiple unmanned air vehicles,” in *IEEE Aerospace Conference*. IEEE, 2008, pp. 1–14.
- [12] P. Hokayem, D. Stipanovic, and M. Spong, “On persistent coverage control,” in *Decision and Control, 2007 46th IEEE Conference on*. IEEE, 2008, pp. 6130–6135.
- [13] Y. Elmaliach, A. Shiloni, and G. Kaminka, “A realistic model of frequency-based multi-robot polyline patrolling,” in *Proceedings of the 7th international joint conference on Autonomous agents and multiagent systems-Volume 1*. International Foundation for Autonomous Agents and Multiagent Systems, 2008, pp. 63–70.
- [14] Y. Elmaliach, N. Agmon, and G. Kaminka, “Multi-robot area patrol under frequency constraints,” in *Robotics and Automation, 2007 IEEE International Conference on*. IEEE, 2007, pp. 385–390.
- [15] C. Cassandras, Y. Wardi, C. Panayiotou, and C. Yao, “Perturbation analysis and optimization of stochastic hybrid systems,” *European Journal of Control*, vol. 16, no. 6, pp. 642–664, 2010.
- [16] Y. Wardi, R. Adams, and B. Melamed, “A unified approach to infinitesimal perturbation analysis in stochastic flow models: the single-stage case,” *IEEE Trans. on Automatic Control*, vol. 55, no. 1, pp. 89–103, 2009.
- [17] A. Bryson and Y. Ho, *Applied optimal control*. Wiley New York, 1975.
- [18] M. Egerstedt, Y. Wardi, and H. Axelsson, “Transition-time optimization for switched-mode dynamical systems,” *Automatic Control, IEEE Transactions on*, vol. 51, no. 1, pp. 110–115, 2006.
- [19] M. Shaikh and P. Caines, “On the hybrid optimal control problem: Theory and algorithms,” *IEEE Transactions on Automatic Control*, vol. 52, no. 9, pp. 1587–1603, 2007.
- [20] X. Xu and P. Antsaklis, “Optimal control of switched systems based on parameterization of the switching instants,” *Automatic Control, IEEE Transactions on*, vol. 49, no. 1, pp. 2–16, 2004.
- [21] C. Yao and C. Cassandras, “Perturbation analysis of stochastic hybrid systems and applications to resource contention games,” *Frontiers of Electrical and Electronic Engineering in China*, vol. 6,3, pp. 453–467, 2011.
- [22] C. Cassandras, J. Lygeros, and C. Press, *Stochastic hybrid systems*. CRC/Taylor & Francis, 2007.
- [23] E. Polak, *Optimization: algorithms and consistent approximations*. Springer Verlag, 1997.